Table 1
Demographic features of 160 MG patients

Sex (M/F)	52:108 (1:2.08)
Mean age at onset (range)	40.4 (0.4–78)
Mean age at examination (range)	52.2 (21–82)
Mean duration of illness (range)	12.7 (0.6–44.7)
Mean anti-AChR antibody titer (range) (nmol/l)	85.8 (0–1200)
Seronegative MG	38/160 (23.8%)
Coexistence of thymoma	37/160 (23.1%)
History of myasthenic crisis	22/160 (13.8%)

titis, urticaria, allergic conjunctivitis, food, drug and metal allergies was studied in 160 consecutive MG patients (108 female and 52 male, mean age 52.2, age range 21–82) who visited the Department of Neurology, Kyushu University Hospital from April 2000 to July 2003; and 81 neurological normal controls (48 female and 33 male, mean age 52.8, age range 16–87) who similarly visited our department during March 1998 and February 2000 and who underwent thorough neurological examinations and laboratory tests and were determined to be neurologically normal. Although bronchial asthma includes both allergic and non-allergic bases, we did not specify 'allergic bronchial asthma' because it is difficult to distinguish the two from a self-administered questionnaire. The diagnosis of MG was established when typical clinical symptoms with diurnal fluctuation and/or easy fatigability were present and at least one of the following tests was positive: (1) Edrophonium test (Tensilon test), (2) repetitive nerve stimulation on the facial and/or median nerves, and (3) measurement of anti AChR antibody through radioimmunoassay. Patients also underwent body CT testing in order to verify thymic abnormalities such as hyperplasia and thymoma. Further, we excluded other diseases that can cause symptoms resembling MG; such as Hashimoto's thyroiditis, Graves' disease, thyroid myopathy, ocular myopathy and mitochondrial diseases.

The patients and controls were requested to complete a questionnaire regarding their past and present history of allergic disorders. The questionnaire set out questions as follows: "Have you ever been diagnosed as having allergic conjunctivitis by your doctor? When did it start and how long did it last? Do you still have the symptom at present? What is the possible cause?" The same questions are repeated for other allergic disorders as well. MG patients and the neurological normal controls completed the questionnaire under the same conditions when they first came to see us.

After completion of the questionnaire, it was noted that there was a high prevalence of AC in the MG patients and so they were divided into two groups, patients with AC (AC+) and those without AC (AC−). Both AC+ and AC− groups were evaluated and compared using clinical features such as the coexistence of thymoma, positive testing for anti-AChR antibodies, rates of seronegative MG, rates of ocular MG, which may include orbicularis oculi muscle weaknesses, and past histories of myasthenic crisis.

The frequency of allergic disorders was statistically compared between MG patients and controls using a chi-square test. The chi-square test was also used to compare the frequency of neurological manifestations, thymoma, seronegative MG and myasthenic crisis between AC+ and AC− patients. Yate's correction method was applied to results when any of the expected number was lower than 5. The uncorrected p values (p^{uncorr}) were multiplied by the number of comparisons (×8) to calculate the corrected p values (p^{corr}). The nonparametric Mann–Whitney U-test was applied to determine the statistical significance of the comparisons of anti-AChR antibody titer levels between AC+ and AC− patients.

3. Results

The demographic features of 160 MG patients are summarized in Table 1. Of the total 160 patients, thymoma was found in 37 (23.1%). Thirty-eight (23.8%) patients were free from anti-AChR antibodies and so were classified as having seronegative MG. A history of myasthenic crisis was present in 22 (13.8%) patients.

The frequencies of the various allergic disorders are summarized in Table 2. Compared with controls, MG patients showed a significantly higher percentage of AC

Table 2
Frequencies of allergic disorders in MG patients

	Control (n=81)	MG total (n=149)	MG	
			Non-thymoma (n=115)	Thymoma (n=34)
Bronchial asthma	4 (4.9)	13 (8.1)	11 (8.9)	2 (5.4)
Allergic rhinitis	11 (13.6)	35 (21.9)	29 (23.6)	6 (16.2)
Atopic dermatitis	4 (4.9)	12 (7.5)	11 (8.9)	1 (2.7)
Urticaria	9 (11.1)	24 (15.0)	21 (17.1)	3 (8.1)
Allergic conjunctivitis	6 (7.4)	39 (24.4)*	36 (29.3)*	3 (8.1)
Food allergy	5 (6.2)	17 (10.6)	13 (10.6)	4 (10.8)
Drug allergy	10 (12.3)	24 (15.0)	19 (15.4)	5 (13.5)
Metal allergy	3 (3.7)	11 (6.9)	8 (6.5)	3 (8.1)

The exact number of patients and the percentages (parenthesis) are shown.
* $p^{corr}<0.05$, as compared with controls.

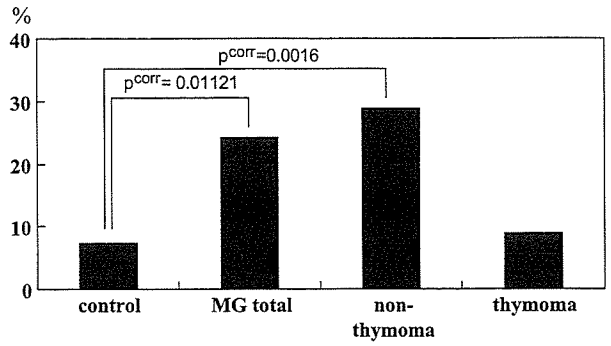

Fig. 1. Frequency of AC in MG patients and controls. MG patients in total have a higher frequency of AC than controls. MG without thymoma has a higher frequency of AC compared to MG with thymoma.

(24.4% in MG and 7.4% in the controls, p^{uncorr}=0.0014, p^{corr}=0.0112) (Table 2). Among MG patients, those with MG and no thymoma showed a significantly higher frequency of AC in comparison with controls (29.3% vs. 7.4%, p^{uncorr}=0.0002, p^{corr}=0.0016) (Fig. 1). There was no significant difference in the frequency of AC between MG cases with thymoma and controls. All other allergic disorders were also present in higher frequencies in MG patients than controls, but the difference was not statistically significant (Table 2).

The 160 MG patients were then subdivided into an AC+ group (39 patients) and an AC− group (121 patients). In the AC+ group, AC preceded MG in 17 cases, MG preceded AC in 15 cases, and both occurred at the same time in four cases, whilst results were unknown in three cases. In the AC+ group, there was a significantly low percentage (7.7%) of thymoma-related MG, in contrast with 28.1% in the AC− group (p=0.016, Fig. 2A). The percentage of seronegative MG was significantly higher in the AC+ group (43.6%) in comparison with the AC− group (17.4%) (p=0.008, Fig. 2B). Anti-AChR antibody titers of seropositive cases were significantly lower in the AC+ group (median 6.8 nmol/l) compared to the AC− group (median 23.6 nmol/l) (p=0.0359, Fig. 2C). The rate of ocular MG tended to be higher in the AC+ group (43.6%) in comparison to the AC− group (28.1%) (p=0.071, Fig. 2D). The incidence of myasthenic crisis was lower in the AC+ group (7.7%) compared with the AC− group (15.7%), but the difference was not statistically significant (Fig. 2E).

4. Discussion

In this study, it was found that the frequency of AC is significantly higher in MG patients, especially in cases of MG without thymoma, in comparison to control patients, and that MG cases with AC have a significantly higher frequency of seronegative MG and lower counts of anti-AChR antibody titers.

The present study has methodological limitations in respect to the accuracy of diagnoses of allergic disorders since such diagnoses are based upon only the questionnaire. However, the types of allergic disorders in the questionnaire investigated were essentially the same as those previously reported in two epidemiological surveys of allergic disorders [18,19], and the phrases of the questions in our study followed one of them [18]. There should be no selection bias because the neurological normal controls and MG patients all completed the same questionnaire in the same setting when they came to our out-patient clinic for their first visit. Moreover, in MG patients, the increase of only AC among eight allergic disorders investigated was highly significant in non-thymoma patients (p^{corr}=0.0016) but not in thymoma patients (p^{corr}>0.05). In addition, the frequency of AC differed significantly between seronegative and

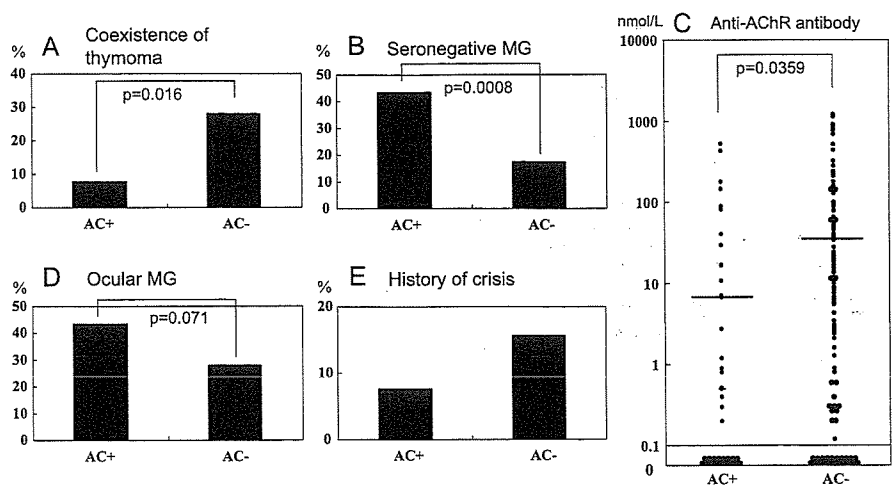

Fig. 2. Comparison of clinical features between MG with AC and MG without AC. (A) Percentage of thymoma associated MG was significantly higher in AC negative cases. (B) Percentage of seronegative MG was significantly higher in AC positive patients. (C) Anti-AChR antibody titer was significantly higher in AC negative patients. Bar indicates median value of each group excluding seronegative cases. (D) Patients without AC had a higher rate of ocular MG. (E) Patients without AC had a higher incidence rate of myasthenic crisis.

seropositive MG patients (p=0.0008). These findings would be difficult to explain if MG patients' concerns about medical problems were the primary cause. Rather, we consider that it reflects some biological features of seronegative non-thymomatous MG patients.

Seronegative MG is frequently encountered in ocular MG cases. As shown in this study, the frequency of ocular MG in the MG patients with AC tended to be higher when compared to the MG cases without AC. This may in part explain the low incidence of crisis in MG patients with AC. The lower rate of thymoma-related MG in the AC+ group also appears to have contributed to a favorable course, since thymoma-related MG was shown to have more severe generalized symptoms than non-thymomatous MG [20]. The rate of seronegative MG in the present study was 23.8%, which is nearly identical to the rate of seronegative MG reported in a nationwide epidemiological survey carried out in Japan in 1987 (23.9% of 963 cases) [21], but somewhat higher than the reported rate of seronegative MG in Caucasians (10–20%) [1,22,23]. Although the reason for such a racial difference of seronegative MG frequency remains to be elucidated, an association of AC with seronegative MG may have some relevance since it was reported that Asians tend to develop atopic tendency more often than Caucasians when living in the same environmental conditions [24].

There are no previous studies that have investigating the association of allergic disorders with MG. In this study, among various allergic disorders, only an increase in AC was statistically significant, yet all other allergic disorders investigated tended to be higher in MG patients than in controls. One possible mechanism for the reasons behind the association of AC with MG is that as ocular manifestations including orbicularis oculi weaknesses are common in MG patients, the conjunctivae may be heavily exposed to such allergens as pollens and house dust mites which could then trigger AC. The increased rate of ocular MG in the AC+ group supports this notion. However, since AC preceded MG in 44% of the MG with AC cases, local exposure to environmental allergens cannot be the sole reason for this association.

It is interesting to note that AC is associated only with MG without thymoma, and not with MG with thymoma. In hyperplastic thymus cases, numerous germinal centers are seen, where CD23 as well as bcl-2 are found to be over-expressed [3,25,26]. These molecules play important roles in preventing germinal center B cells from entering apoptosis, which thereby results in autoantibody production. In allergic disorders, aberrant lymphocyte development in the thymus is considered to play an important role in the occurrence of atopic dermatitis, in which the suppression of lymphocyte apoptosis also leads to the development of allergic reactions [27,28]. Therefore, the second hypothesis for an association between MG and AC is that MG without thymoma and AC may have common disease backgrounds originating from thymic alterations, distinct from that of MG with thymoma lacking germinal centers. This notion is also supported by observations that the frequencies of other allergic disorders also tended to be higher in MG without thymoma than in the controls. Moreover, CD23, a low affinity receptor for IgE, is profoundly related to allergic disorders. The soluble form of CD23 is elevated in allergic diseases as well as in MG [6–10], which also supports the common immunological aberrancy between MG and certain allergic diseases. The production of autoantibodies in thymoma-related MG is likely to be independent from the germinal center, and have an alternative pathway.

To summarize, it was found that there is a significant association of AC with certain forms of MG in cases without thymoma. However, this study should be considered a preliminary one, and an epidemiological survey accompanied by laboratory testing for allergies will be required in the future to clarify such an association. Nonetheless, MG may predispose patients to AC through the heavy exposure of allergens to the conjunctivae due to orbicularis oculi weaknesses, in which case special care in respect to air-borne allergens appears warranted.

References

[1] Lewis RA, Selwa JF, Lisak RP. Myasthenia gravis: immunological mechanisms and immunotherapy. Ann Neurol 1995;37(Suppl. 1): S51–62.
[2] Hoch W, McConville J, Helms S, Newsom-Davis J, Melms A, Vincent A. Auto-antibodies to the receptor tyrosine kinase MuSK in patients with myasthenia gravis without acetylcholine receptor antibodies. Nat Med 2001;7:365–8.
[3] Murai H, Hara H, Hatae T, Kobayashi T, Watanabe T. Expression of CD23 in the germinal center of thymus from myasthenia gravis patients. J Neuroimmunol 1997;76:61–9.
[4] Gonzalez-Molina A, Spiegelberg HL. Binding of IgE myeloma proteins to human cultured lymphoblastoid cells. J Immunol 1976; 117:1838–45.
[5] Yukawa K, Kikutani H, Owaki H, Yamasaki K, Yokota A, Nakamura H, et al. A B cell-specific differentiation antigen, CD23, is a receptor for IgE (Fc epsilon R) on lymphocytes. J Immunol 1987;138:2576–80.
[6] Bansal A, Roberts T, Hay EM, Kay R, Pumphrey RS, Wilson PB. Soluble CD23 levels are elevated in the serum of patients with primary Sjogren's syndrome and systemic lupus erythematosus. Clin Exp Immunol 1992;89:452–5.
[7] Bansal AS, Ollier W, Marsh MN, Pumphrey RS, Wilson PB. Variations in serum sCD23 in conditions with either enhanced humoral or cell-mediated immunity. Immunology 1993;79:285–9.
[8] Chomarat P, Briolay J, Banchereau J, Miossec P. Increased production of soluble CD23 in rheumatoid arthritis, and its regulation by interleukin-4. Arthritis Rheum 1993;36:234–42.
[9] Tanaka A, Ohashi Y, Nakai Y. Decrease of serum levels of soluble CD23 during immunotherapy in patients with perennial allergic rhinitis. Ann Otol Rhinol Laryngol 1999;108:193–200.
[10] Tsicopoulos A, Joseph M. The role of CD23 in allergic disease. Clin Exp Allergy 2000;30:602–5.
[11] Gross WL. Churg-Strauss syndrome: update on recent developments. Curr Opin Rheumatol 2002;14:11–4.

[12] Kira J, Yamasaki K, Kawano Y, Kobayashi T. Acute myelitis associated with hyperIgEemia and atopic dermatitis. J Neurol Sci 1997;148:199–203.
[13] Kira J, Kawano Y, Yamasaki K, Tobimatsu S. Acute myelitis with hyperIgEaemia and mite antigen specific IgE: atopic myelitis. J Neurol Neurosurg Psychiatry 1998;64:676–9.
[14] Kira J, Kawano Y, Horiuchi I, Yamada T, Imayama S, Furue M, et al. Clinical, immunological and MRI features of myelitis with atopic dermatitis (atopic myelitis). J Neurol Sci 1999;162:56–61.
[15] Horiuchi I, Yamasaki K, Osoegawa M, Ohyagi Y, Okayama A, Kurokawa T, et al. Acute myelitis after asthma attacks with onset after puberty. J Neurol Neurosurg Psychiatry 2000;68:665–8.
[16] Ochi H, Murai H, Osoegawa M, Minohara M, Inaba S, Kira J. Juvenile muscular atrophy of distal upper extremity associated with airway allergy: two cases successfully treated by plasma exchange. J Neurol Sci 2003;206:109–14.
[17] Gazerani P, Pourpak Z, Ahmadiani A, Hemmati A, Kazemnejad A. A correlation between migraine, histamine and immunoglobulin e. Scand J Immunol 2003;57:286–90.
[18] Kira J, Osoegawa M, Horiuchi I, Murai H, Minohara M, Ohyagi Y, et al. History of allergic disorders in common neurologic diseases in Japanese patients. Acta Neurol Scand 2002;105:215–20.
[19] Yamazaki M, Shogo S, Taniwaki H, Nagaoka K, Asada Y, Kai-Ping S, et al. Allergy histories of Brazilian residents of Japanese descent in Japan. Nippon Koshu Eisei Zasshi 1995;42:525–33 [in Japanese].
[20] Robertson NP, Deans J, Compston DA. Myasthenia gravis: a population based epidemiological study in Cambridgeshire, England. J Neurol Neurosurg Psychiatry 1998;65:492–6.
[21] Ide Y, Takamori M. Japanese clinical statistical data of patients with myasthenia gravis. Nippon Rinsho 1992;50(Suppl.):186–93 [in Japanese].
[22] Engel AG. Myasthenia gravis and myasthenic syndromes. Ann Neurol 1984;16:519–34.
[23] Vincent A, Newsom-Davis J. Acetylcholine receptor antibody as a diagnostic test for myasthenia gravis: results in 153 validated cases and 2967 diagnostic assays. J Neurol Neurosurg Psychiatry 1985;48: 1246–52.
[24] Leung RC, Carlin JB, Burdon JG, Czarny D. Asthma, allergy and atopy in Asian immigrants in Melbourne. Med J Aust 1994;161:418–25.
[25] Onodera J, Nakamura S, Nagano I, Tobita M, Yoshioka M, Takeda A, et al. Upregulation of Bcl-2 protein in the myasthenic thymus. Ann Neurol 1996;39:521–8.
[26] Shiono H, Fujii Y, Okumura M, Takeuchi Y, Inoue M, Matsuda H. Failure to down-regulate Bcl-2 protein in thymic germinal center B cells in myasthenia gravis. Eur J Immunol 1997;27:805–9.
[27] Ohta K, Yamashita N. Apoptosis of eosinophils and lymphocytes in allergic inflammation. Int Arch Allergy Immunol 1999;104:14–21.
[28] Simon HU. Apoptosis in inflammatory diseases. Int Arch Allergy Immunol 1999;118:261–2.

ELSEVIER

Journal of the Neurological Sciences 227 (2004) 39–47

Journal of the Neurological Sciences

www.elsevier.com/locate/jns

Effect of immunotherapy in myelitis with atopic diathesis

Hiroyuki Murai[a,1], Hajime Arahata[a,1], Manabu Osoegawa[a], Hirofumi Ochi[a], Motozumi Minohara[a], Takayuki Taniwaki[a], Shozo Tobimatsu[b], Futoshi Mihara[c], Yuko Tsuruta[a,d], Shoichi Inaba[d], Jun-ichi Kira[a,*]

[a]*Department of Neurology, Neurological Institute, Graduate School of Medical Sciences, Kyushu University, Fukuoka 812-8582, Japan*
[b]*Department of Clinical Neurophysiology, Neurological Institute, Graduate School of Medical Sciences, Kyushu University, Fukuoka, Japan*
[c]*Division of Neuroradiology, Department of Radiology, Graduate School of Medical Sciences, Kyushu University, Fukuoka, Japan*
[d]*Blood Transfusion Service, Kyushu University Hospital, Fukuoka, Japan*

Received 2 April 2004; received in revised form 6 August 2004; accepted 9 August 2004
Available online 2 October 2004

Abstract

Objective: A recent nationwide survey of myelitis with atopic diathesis in Japan disclosed that the disease frequently shows a chronic persistent course. A neuropathological study of the spinal cord also revealed chronic active inflammation. Since the effects of various immunotherapies have not been studied extensively in this condition, we evaluated the efficacies of various immunotherapies in patients with myelitis with atopic diathesis.

Patients and methods: Forty-two treatments in 26 patients with myelitis with atopic diathesis were retrospectively analyzed. One of the following therapies was administered: (1) corticosteroids (CS) (pulse therapy followed by oral administration with gradual tapering); (2) intravenous immunoglobulin (IVIG) (400 mg/kg/day for 5 consecutive days); (3) plasma exchanges (PE); or (4) PE followed by IVIG or CS (PE+IVIG/CS). The therapeutic efficacies were evaluated by thorough neurological examination and laboratory tests including MRI, somatosensory evoked potentials (SEPs) and motor evoked potentials (MEPs).

Results: Objective neurological findings improved in 89% of the PE group and 90% of the PE+IVIG/CS group, compared with only 72% of the CS and 60% of the IVIG groups. Improvement determined by laboratory tests was seen in 57% of the PE and 57% of the PE+IVIG/CS groups, compared with only 15% of the CS and none of the IVIG groups. Thus, the improvement rate determined by laboratory tests was significantly greater for therapies including PE than for those without PE ($p=0.0187$).

Conclusions: These data suggest that immunotherapy is effective in myelitis with atopic diathesis despite a chronic persistent course, and that PE is the most beneficial immunotherapy.

Keywords: Myelitis; Atopy; Treatment; Corticosteroid; Plasma exchange; IVIG

1. Introduction

We have previously reported the occurrence of myelitis with atopic diathesis in Japanese patients [1–3]. Following our reports, several similar cases have been reported in the Japanese literature [4–6], and a recent nationwide survey disclosed the widespread occurrence of myelitis with atopic diathesis (atopic myelitis) throughout Japan [7].

Atopy is generally considered to be a helper type 2 (Th2) disease, in which type 2 cytokines, such as IL-4, IL-5, IL-6 and IL-13, play critical roles in the induction of inflammation [8]. Pathological studies on biopsied specimens of the spinal cord from patients with atopic myelitis revealed eosinophil infiltration as well as deposition of activated eosinophil products, such as eosinophil cationic protein (ECP), in the lesions [9,10]. Moreover, amounts of IgE in the cerebrospinal fluid (CSF) were found to be increased in

* Corresponding author. Tel.: +81 92 642 5340; fax: +81 92 642 5352.
E-mail address: kira@neuro.med.kyushu-u.ac.jp (J. Kira).
[1] These authors contributed equally to this study.

0022-510X/$ - see front matter © 2004 Elsevier B.V. All rights reserved.
doi:10.1016/j.jns.2004.08.001

this condition [7]. These findings suggest that an inflammatory mechanism driven by Th2 cells may be operative, even in the central nervous system (CNS), similar to other atopic disorders.

Clinical studies on myelitis with atopic diathesis have revealed that it frequently shows a chronic persistent course, and that MRI lesions also tend to persist for years despite their small size [1–3,7,10]. These clinical and neuroimaging features as well as neuropathological findings suggest that the mechanism for myelitis with atopic diathesis is possibly distinct from the autoimmune mechanism proposed for multiple sclerosis (MS). Thus, the response to various immunotherapies in this condition may also be distinct from those in MS. Since there are no reports that extensively examine the effects of immunotherapy in this condition, we retrospectively evaluated the treatment responses in patients with atopic myelitis by neurological and laboratory examinations.

2. Patients and methods

2.1. Patients

Myelitis with atopic diathesis (atopic myelitis) was defined as myelitis of unknown cause with either (1) hyperIgEemia and allergen-specific IgE positivity against common allergens, such as *Dermatophagoides pteronyssinus* (*D. pteronyssinus*), *Dermatophagoides farinae* (*D. farinae*) and cedar pollen, or (2) coexistent atopic diseases, as described previously [7]. Atopic disorders such as atopic dermatitis, bronchial asthma, allergic rhinitis and food allergies, which involve atopic mechanisms, were regarded as coexistent atopic diseases [11]. Cases showing multiple brain white matter lesions which met McDonald's diagnostic criteria for multiple sclerosis [12] were excluded from the study.

Twenty-six patients with atopic myelitis who had been admitted to the Department of Neurology at Kyushu University Hospital from 1992 to 2003 were enrolled in this study. The study was approved by the Institutional Review Board of Kyushu University Hospital. The demographic features of the patients are summarized in Table 1. The patients consisted of 13 males and 13 females (1:1). The mean age at treatment was 36.6±11.2 years (mean± S.D.) (range, 15–58), and the mean duration of the disease at treatment was 25.8±26.8 months (mean±S.D.) (range, 1–132). The mode of onset and disease course before any treatment of the 26 patients were: acute and persistent in 7 (27.0%), acute and fluctuating in 6 (23.1%), acute and step-wise progression in 4 (15.4%), subacute and fluctuating in 2 (7.7%), subacute and step-wise progression in 1 (3.8%) and slowly progressive in 6 (23.1%).

Atopic disorders were present in 80.8% of patients: allergic rhinitis in 10/26 (38.5%), atopic dermatitis in 9/26 (34.6%), bronchial asthma in 4/26 (15.4%) and a food allergy in 5/26 (19.2%). Eosinophilia was found in 11/26 patients (42.3%) and hyperIgEemia in 19/26 (73.1%) at the time of the initial treatment. Twenty-four of the twenty six patients (92.3%) had specific IgE against *D. pteronyssinus*, 22/26 (84.6%) against *D. farinae* and 18/26 (69.2%) against cedar pollen. CSF examination revealed cell counts of 1.0±1.3/μl (mean±S.D.) (range, 0–15/μl) and a total protein level of 35.6±17.9 mg/dl (mean±S.D.) (range, 16–106 mg/dl). CSF pleocytosis (>5/μl) was found in 6/26 patients (23.1%), and an increased protein level (>40 mg/dl) was found in 8/26 (30.8%).

2.2. Treatments

One of the following treatments was administered after informed consent was obtained from each patient, and the efficacies of the treatments were evaluated by clinical examinations as well as laboratory tests, and analyzed retrospectively: (1) corticosteroids (CS); (2) intravenous immunoglobulin (IVIG); (3) plasma exchanges (PE); or (4) PE followed by either IVIG or CS (PE+IVIG/CS). CS were administered by intravenous injection of methylprednisolone 1000 mg/day for 3 days followed by oral prednisolone (initial dose of 60 mg/day) with gradual tapering. Patients assigned to IVIG treatment received intravenous infusions of gammaglobulin (Kenketsu Glovenin-I-Nichiyaku, Takeda Chemical Industries) at a dose of 400 mg/kg/day for 5 consecutive days. PE was performed three times using Spectra (COBE) at 2- to 3-day intervals, and the entire procedure was carried out in a closed circuit. Briefly, the patient's blood was obtained from a forearm vein and delivered to a single-stage channel where centrifugation separated the blood into plasma and blood cells. The blood cells were then returned to the patient's vein together with a replacement solution consisting of 2.3% albumin. Plasma (40 ml/kg) was replaced in each procedure. In the patients who received PE+IVIG or PE+CS treatment, either IVIG or CS was performed 1–3 weeks after the PEs had been completed. The procedures for each treatment were the same as described above.

2.3. Evaluation of treatments

The clinical effects of the treatments were evaluated objectively by neurological examination by expert neurologists before and 2–4 weeks after each treatment. Improvement in any neurological sign was considered to be an indication of effectiveness. Kurtzke's expanded disability status scale score (EDSS) [13] and the Scripps neurological rating scale (NRS) [14] were also evaluated. MRI examinations including a dual-echo, proton density, T2-weighted spin-echo series (TR=2000 ms, TE=90 ms) and T1-weighted spin-echo series (TR=600 ms, TE=20 ms) with and without gadolinium enhancement were performed before and after the treatments as described previously [3], and the treatment effects were evaluated by expert neuroradiologists without knowledge of the treatment modality.

Table 1
Demographic features of atopic myelitis patients

Case	Age	Sex	Atopic diathesis									SL	CSF		Tx	Improvement	
			AD	BA	AR	FA	Eo	IgE	DP	DF	CP		Cell	Prot		NE	Lab
1	25	F	–	–	+	–	–	+	+	+	+	MT	1	21	PE	+	+
2	21	M	–	+	–	–	+	+	+	+	–	C5	2	25	CS	+	–
3	58	F	–	–	+	–	+	+	+	+	+	C1	1	16	CS	+	Wor
4	43	M	–	+	–	+	–	–	+	+	+	C5	4	51	PE	+	–
5	32	M	+	–	–	–	–	–	+	+	+	L1	0	43	PE	+	–
6	33	F	+	–	+	–	–	+	+	–	+	C5	0	26	PE+IVIG	+	–
7	27	M	–	–	+	+	+	+	+	+	–	C3	2	20	CS	+	–
	28											C3	15	56	PE+IVIG	+	–
	30											UT	ND	ND	IVIG	–	ND
	31											UT	ND	ND	PE+IVIG	+	–
	32											LT	0	70	PE+CS	–	+
8	38	F	+	–	–	–	+	+	+	+	+	C6	1	25	PE	–	+
9	48	F	–	–	+	+	–	–	–	–	+	C6	ND	ND	CS	+	–
10	48	M	–	–	+	–	+	+	+	+	–	C6	1	106	CS	+	–
11	24	F	+	–	–	+[a]	–	–	–	–	–	C5	3	17	CS	+	–
12	22	F	–	+	–	–	–	–	+	+	+	L5	3	52	CS	–	ND
	23											L5	1	52	IVIG	–	–
13	31	M	+	–	–	–	+	–	+	+	+	C5	0	20	CS	+	–
14	48	M	+	–	–	–	+	+	+	+	+	LT	5	24	IVIG	+	–
	48											LT	1	24	PE	+	+
	46											MT	0	29	CS	+	+
15	50	F	+	–	–	–	–	+	+	+	+	C6	1	31	CS	+	ND
16	51	M	–	+	+	–	–	+	+	+	–	C3	ND	ND	IVIG	+	–
	51											C3	1	28	PE	+	–
17	34	F	–	–	+	–	+	+	+	+	+	LT	10	35	CS	+	ND
	37											MT	1	27	PE+IVIG	+	–
	39											MT	0	38	PE+IVIG	+	ND
18	54	F	–	–	+	–	–	+	+	+	+	C4	2	35	PE+IVIG	–	–
	54											C4	9	49	PE+CS	+	+
19	41	F	–	–	+	+	–	–	+	+	+	C3	ND	ND	PE	+	Wor
	41											C3	5	26	CS	–	–
20	18	F	+	–	–	–	+	+	+	+	+	C4	8	19	CS	+	–
21	35	F	+	–	–	–	–	+	+	+	–	C6	9	25	PE+CS	–	+
22	37	M	–	–	–	–	+	+	+	+	+	C3	5	30	CS	+	ND
	40											C3	ND	ND	PE	+	ND
23	42	M	–	–	–	–	+	+	+	+	+	C6	1	53	CS	+	+
	43											C6	12	39	PE	+	+
	44											C6	ND	ND	IVIG	+	–
24	33	M	–	–	–	–	–	+	+	+	+	UT	3	29	CS	–	–
25	15	M	–	–	–	–	–	+	+	–	–	C5	1	46	CS	–	–
	16											C5	0	32	PE+IVIG	+	+
26	25	M	–	–	–	–	–	+	+	+	–	LT	1	26	CS	+	ND

Age=age at treatment; AD=atopic dermatitis; BA=bronchial asthma; AR=allergic rhinitis; FA=food allergy; Eo=eosinophilia (>4%); IgE=cases of hyperIgEemia in which total IgE exceeded the normal limit (*N*: <240 IU/ml); DP=*Dermatophagoides pteronyssinus*-specific IgE (N: <0.34 IU/ml); DF=*Dermatophagoides farinae*-specific IgE (*N*: <0.34 IU/ml); CP=cedar pollen-specific IgE (*N*: <0.34 IU/ml); SL=clinically estimated level of the spinal cord lesion: C=cervical, UT=upper thoracic, MT=middle thoracic, LT=lower thoracic, L=lumbar; CSF=cerebrospinal fluid: Cell=number of cells (/μl), Prot=protein concentration (mg/dl); Tx=treatment: CS=corticosteroids, IVIG=intravenous immunoglobulin, PE=plasma exchanges; Improvement=improvement detected in each patient: NE=improvement detected by neurological examination, Lab=improvement supported by MRI and/or electrophysiological studies, +=improved, –=unchanged, ND=not done, Wor=worsened.

[a] This patient was allergic to egg white and positive for allergen-specific IgE against egg white protein.

Motor evoked potentials (MEPs) with transcranial magnetic stimulation were recorded as previously described [15]. The upper limb MEPs were recorded from the abductor pollicis brevis muscle. To stimulate the hand motor area, the center of the eight-shaped coil was placed over a point 2 cm anterior to either C3 or C4 (International 10–20 System). To stimulate the cervical root, the center of the coil was placed on the posterior neck over the 7th cervical spinous process. The lower limb MEPs were recorded from the abductor hallucis muscle. To stimulate the leg motor area, the coil was positioned over the vertex. Magnetic stimulation to the lumbar root was performed by placing the center of the coil over the 4th lumbar spinous process. Somatosensory evoked potentials (SEPs) were analyzed following electric stimulation of the median nerve and tibial nerve [15]. The peak amplitudes of the far-field

P14 and the cortical N20, and the peak-to-peak amplitude of P25, P30 and N35 were measured. The latency of each peak was also measured. On follow-up studies, the evoked potentials were considered to be improved when unevoked potentials became evoked or when a delayed peak shifted forward to fall within the normal limits.

2.4. Statistical analysis

Wilcoxon signed-ranks test was applied to determine the statistical significance of the changes in the EDSS and NRS scores, the percentage of peripheral eosinophils, and the amounts of total IgE and allergen-specific IgE against *D. pteronyssinus*, *D. farinae* and cedar pollen. Kruskal–Wallis rank test was used for comparison of the EDSS and NRS scores and the disease duration among the four treatment groups. Chi-square test, or Fisher's exact test when the Chi-square test was not fulfilled, was used for statistical analyses of comparison of improvement rates by treatment.

3. Results

3.1. Pretreatment status

The 26 patients received a total of 42 treatments. Disease duration in terms of months at the time of treatment was significantly different among the four treatment groups (CS: 19.2±30.8; IVIG: 25.4±11.9; PE: 20.9±16.4; and PE+IVIG/CS: 42.5±27.5; p=0.0374). Of the 42 events, 40 (95.2%) showed sensory impairment, such as hypesthesia, hypalgesia and a decrease in vibration sense, and 36 (85.7%) had a motor impairment, such as muscle weakness, hyperreflexia and pathological reflexes on neurological examination (details are shown in Table 2). Five patients (11.9%) were diagnosed as having sphincter disturbance by uroflowmetry analysis. The pretreatment EDSS scores were 3.54±0.98 (mean±S.D.) (range, 2.0–7.5), and these differed significantly among the four treatment groups (p=0.0031) (Table 3). The pretreatment NRS scores were 83.12±8.20 (mean±S.D.) (range, 66–94), and these also differed significantly among the four groups (p=0.0151). Clinically estimated main lesions existed in the cervical spinal cord in 27/42 cases (64.3%), in the thoracic spinal cord in 12/42 (28.6%) and in the lumbar spinal cord in 3/42 (7.1%).

On T2-weighted MRI images (T2WI), localized spinal cord lesions of high signal intensity were detected in 22/40 pretreatment scans (55.0%). Gadolinium-enhancement of the lesions was observed in 8 of these 22 pretreatment lesions (36.4%). Cervical spinal cord lesions were most frequently observed among the spinal cord lesions on MRI (18/22, 81.8%), while 8/22 (36.4%) were in the thoracic spinal cord and 0/22 were in the lumbar spinal cord. Abnormalities in MEPs were disclosed in 8/35 cases

Table 2
Effect of each treatment on neurological symptoms and signs

	CS		IVIG		PE		PE+IVIG/CS		Total	
	Pre	Imp	Pre	Imp	Pre	Imp	Pre	Imp	Pre	Imp
Sensory										
Hypesthesia	17	12	4	2	6	6	10	5	37	25
Hypalgesia	5	2	1	0	3	2	3	1	12	5
Decrease in vibration sense	12	7	3	1	4	2	9	3	28	13
Decrease in position sense	2	2	0	0	0	0	2	0	4	2
Pseudoathetosis	0	0	0	0	0	0	0	0	0	0
Girdle sensation	3	2	1	0	1	1	3	2	8	5
Lhermitte sign	2	1	0	0	0	0	0	0	2	1
Sensory total	17	13	5	3	8	7	10	6	40	28
(% of improvement)		76.5		60.0		78.5		60.0		70.0
Motor										
Muscle weakness	13	9	3	1	6	4	10	8	32	22
Muscle atrophy	0	0	0	0	0	0	0	0	0	0
Spasticity	5	2	0	0	1	0	3	0	9	2
Hyperreflexia	8	0	2	0	4	1	6	2	20	3
Hyporeflexia	1	1	0	0	0	0	0	0	1	1
Pathological reflex	6	1	1	1	2	0	4	0	13	2
Gait	5	3	0	0	0	0	7	3	12	6
Motor total	14	9	3	1	6	4	9	8	36	25
(% of improvement)		64.3		33.3		66.7		88.9		69.4
Autonomic										
Sphincter disturbance	2	2	0	0	0	0	3	2	5	4
Autonomic total	2	2	0	0	0	0	3	2	5	4
(% of improvement)		100.0		–		–		66.7		80.0
Total	18	13	5	3	9	8	10	9	42	33
(% of improvement)		72.2		60.0		88.9		90.0		78.6

CS=corticosteroids; IVIG=intravenous immunoglobulin; PE=plasma exchanges. Pre=number of patients who had the symptoms/signs before treatment. Imp=number of patients whose symptoms/signs improved after treatment. UE=upper extremities; LE=lower extremities.

Table 3
Effect of each treatment on EDSS and NRS

	CS		IVIG		PE		PE+IVIG/CS		Total	
	Pre	Post	Pre	Post	Pre	Post	Pre	Post	Pre	Post
EDSS										
Mean	3.44	3.19	3.40	3.40	2.83	2.56	4.40	4.00	3.54	3.27
S.D.	0.55	0.62	0.55	0.55	0.56	0.58	1.43	1.43	0.98	0.98
Rate of improvement (%)	6/18 (33.3)		0/5 (0.0)		3/9 (33.3)		5/10 (50.0)		14/42 (33.3)	
p	0.0235		NA		>0.1		0.0384		0.0007	
NRS										
Mean	85.72	89.50	83.20	84.40	86.22	91.44	75.60	81.30	83.12	87.36
S.D.	7.47	5.24	11.35	12.40	4.74	3.36	6.15	6.57	8.20	7.33
Rate of improvement	12/18 (66.7)		3/5 (60.0)		8/9 (88.9)		10/10 (100.0)		33/42 (78.6)	
p	0.0023		>0.1		0.0115		0.005		<0.0001	

CS=corticosteroids; IVIG=intravenous immunoglobulin; PE=plasma exchanges. Pre=pre-treatment; Post=post-treatment. S.D.=Standard deviation; NA=not applicable.

(22.9%) in the upper limbs and 10/36 (27.8%) in the lower limbs. Abnormal findings in SEPs were observed in 5/33 cases (15.2%) in the upper limbs and 17/32 (53.1%) in the lower limbs.

3.2. Effects of treatments on the neurological symptoms and signs

3.2.1. Overall effects of treatments

Overall improvement seen by neurological examination was demonstrated in 33/42 treatments (78.6%) (Table 2). Among the neurological signs, sensory signs improved in 28/40 treatments (70.0%), motor signs in 25/36 (69.4%) and autonomic signs in 4/5 (80.0%). EDSS scores improved in 14/42 treatments (33.3%) (Table 3). The pretreatment EDSS scores of 3.54 ± 0.98 were significantly reduced to 3.27 ± 0.98 after the treatments ($p=0.0007$). NRS scores improved in 33/42 treatments (78.6%) (Table 3). The pretreatment NRS scores were 83.12 ± 8.20 and they significantly increased to 87.36 ± 7.33 after the treatments ($p<0.0001$).

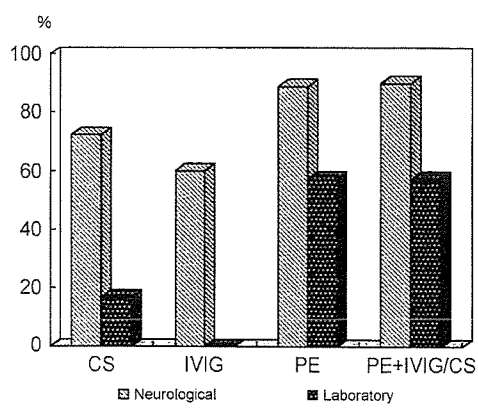

Fig. 1. The efficacy of each treatment for atopic myelitis. The rates of improvement evaluated by neurological examination and laboratory tests are shown. The number of events (treatments) for the neurological examination and laboratory tests were 18 and 13 for CS, 5 and 3 for IVIG, 9 and 7 for PE and 10 and 7 for PE+IVIG/CS, respectively.

3.2.2. Effects of each treatment

Effects of each treatment are summarized in Tables 2 and 3. EDSS score did not change in the IVIG group, but improved significantly in the CS and in PE+IVIG/CS groups. EDSS improvement did not reach statistical significance in just the PE group. NRS scores improved in

Table 4
Overall effect of treatment on MRI and evoked potential findings

MRI changes		
T2-weighted Images (T2WI)		
Disappearance of T2-high intensity lesion	1/13	(7.7%)
Reduction of T2-high intensity lesion	3/13	(23.1%)
Increase of area on T2WI	1/13	(7.7%)
Newly appeared area on T2WI	0	
Gd-enhanced T1-weighted images		
Disappearance of Gd-enhanced lesion	2/5	(40.0%)
Reduction of Gd-enhanced lesion	1/5	(20.0%)
Newly appeared Gd-enhanced lesion	1	
Overall effects		
Improved	6/13	(46.2%)
Unchanged	5/13	(38.5%)
Worsened	2/13	(15.4%)
Evoked potential changes		
MEPs upper limbs		
Improved	2/6	(33.3%)
Unchanged	4/6	(66.7%)
Worsened	0/6	(0.0%)
MEPs lower limbs		
Improved	1/7	(14.3%)
Unchanged	6/7	(85.7%)
Worsened	0/7	(0.0%)
SEPs upper limbs		
Improved	0/2	(0.0%)
Unchanged	2/2	(100.0%)
Worsened	0/2	(0.0%)
SEPs lower limbs		
Improved	3/5	(60.0%)
Unchanged	2/5	(40.0%)
Worsened	0/5	(0.0%)
Overall effects		
Improved	6/8	(75.0%)
Unchanged	2/8	(25.0%)
Worsened	0/8	(0.0%)

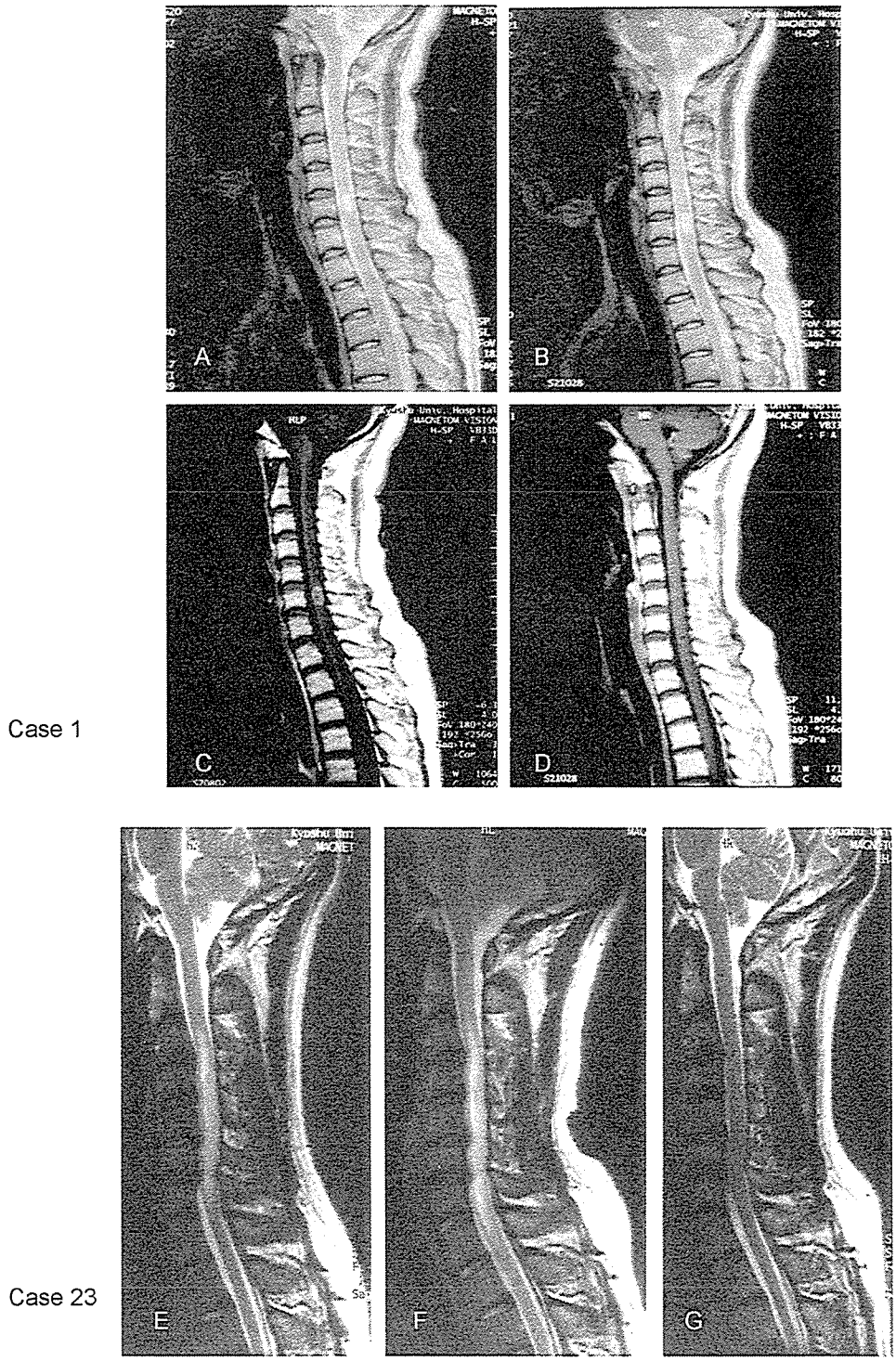

Fig. 2. Representative cases showing improvement on MRI. Case 1: (A) T2-weighted MRI before PE; (B) T2-weighted MRI after PE; (C) T1-weighted MRI with gadolinium enhancement before PE; and (D) T1-weighted MRI with gadolinium enhancement after PE. A T2-high intensity lesion is located at the C6 spine level and is enhanced by gadolinium. After the PE treatment, the enhancement has disappeared although the T2-high intensity lesion is unchanged. Case 23: (E) T2-weighted MRI before CS; (F) T2-weighted MRI after CS and before PE; and (G) T2-weighted MRI after PE. A T2-high lesion is seen at the C3-7 spine levels. After the treatment with CS, the lesion is not improved, but it disappears after performing PE.

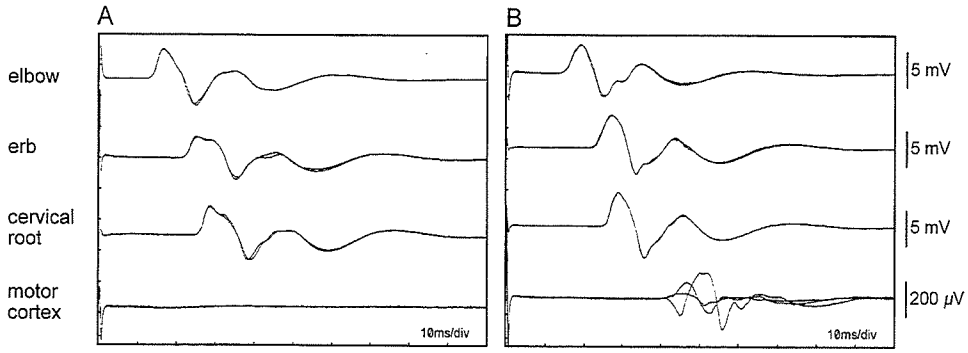

Fig. 3. A representative case showing improvement in the MEP of the left upper limb (Case 8). (A) Before PE treatment; and (B) After PE treatment. The MEP of the motor cortex stimulation that was not evoked before treatment becomes evoked after performing PE.

all four treatment groups but the improvement did not reach the statistical significance in the IVIG group. In summary, objective neurological findings improved in 88.9% of the PE and 90.0% of the PE+IVIG/CS groups, compared with only 72.2% of the CS and 60.0% of the IVIG groups (Fig. 1). The improvement rates on neurological examination and in the EDSS scores were higher for treatments including PE (PE and PE+IVIG/CS groups) than for those without PE (CS and IVIG groups) (17/19, 89.5% vs. 16/23, 69.6%, p=0.118 on neurological findings; 8/19, 42.1% vs. 6/23, 26.1%, p=0.273 in EDSS scores; and 18/19, 94.7% vs. 15/23, 65.2% p=0.0203 in NRS scores). The EDSS scores for treatments including PE (PE group and PE+IVIG/CS group) were significantly reduced from 3.66±0.13 to 3.32±0.13 (p=0.0094), and the NRS scores were significantly elevated from 83.12±8.20 to 87.36±7.33 (p<0.0001).

3.3. Effects of treatments on laboratory findings

3.3.1. Effects of treatments on spinal cord MRI findings

High signal intensity lesions on T2-weighted MRI disappeared in 1/13 treatments (7.7%) and the size was reduced in 3/13 (23.1%) (Table 4). In one treatment (5.9%), T2-weighted MRI revealed an increase in the high signal intensity area. On gadolinium-enhanced T1-weighted images, gadolinium-enhanced lesions disappeared in 2/5 treatments (40.0%) and the lesion size was reduced in 1/5 (25.0%). In one case whose pre-treatment MRI lesion was not enhanced by gadolinium, an enhanced lesion newly appeared after the treatment. Representative cases in which MRI improvements were observed are shown in Fig. 2. Overall, improvement after immunotherapies was observed on MRI in 6/13 (46.2%).

3.3.2. Effects of treatments on the evoked potentials

Electrophysiologically, improvements in MEPs were observed in 2/6 treatments (33.3%) for the upper limbs and 1/7 (14.3%) for the lower limbs (Table 4). Three of five treatments (60%) showed improvements in SEPs for the lower limbs, compared with 0/2 for the upper limbs. A representative case showing MEP improvement is shown in Fig. 3. Overall, improvement in the evoked potentials after immunotherapies was seen in 6/8 (75%).

3.3.3. Effects of each treatment on laboratory examinations (MRI and/or EPs)

Improvements supported by laboratory examinations were seen in 4/7 (57.1%) of the PE group (of these 7 events, neurological improvement was seen in 6) and 4/7 (57.1%) of the PE+IVIG/CS group (of these 7 events, neurological improvement was seen in 6), compared with only 2/13 (15.4%) of the CS group (of these 13 events, neurological improvement was seen in 11) and 0/3 of the IVIG group (of these 3 events, neurological improvement was seen in 2).

Table 5
Effect of each treatment on blood tests

	CS		IVIG		PE		PE+IVIG/CS		Total	
	Pre	Post	Pre	Post	Pre	Post	Pre	Post	Pre	Post
Eosonophil (%)	5.98	1.76	3.17	3.27	3.6	2.99	5.39	4.48	5.04	2.85
p	0.0052		NA		>0.1		>0.1		0.049	
Total IgE (IU/ml)	2058	1024	229	230	2063	2011	833	1202	1355	1115
p	>0.1		NA		>0.1		>0.1		>0.1	
D. pteronyssinus IgE (IU/ml)	53.4	46.3	22.6	21.4	36.4	35.7	45.2	48.0	42.7	43.7
p	>0.1		NA		>0.1		>0.1		>0.1	
D. farinae IgE (IU/ml)	40.7	36.5	20.1	20.7	35.6	35.9	40.3	43.9	38.4	38.9
p	>0.1		NA		>0.1		>0.1		>0.1	
Cedar pollen IgE (IU/ml)	9.6	9.1	<0.34	<0.34	4.8	4.1	29.4	28.0	17.2	16.3
p	>0.1		NA		>0.1		>0.1		>0.1	

CS=corticosteroids; IVIG=intravenous immunoglobulin; PE=plasma exchanges. Pre=pre-treatment; Post=post-treatment. NA=not applicable.

The improvement rate on laboratory examinations was significantly greater for treatments including PE (PE and PE+IVIG/CS groups) than for those without PE (CS and IVIG groups) (8/14, 57.1% vs. 2/16, 12.5%, p=0.0187).

3.3.4. Effects of treatments on blood tests

Changes in hematological examinations are summarized in Table 5. Overall, the percentage of eosinophils fell significantly from 5.04 to 2.85 (p=0.049), and among the immunotherapies, reduction was significant only in treatments with CS. The total and allergen-specific IgEs did not change significantly.

4. Discussion

In the present study, we have disclosed for the first time the responses of atopic myelitis to various immunotherapies. In our series, three-quarters of patients with atopic myelitis responded, more or less, to immunotherapies; indicating that spinal cord dysfunction in this condition is partly reversible, although most of the patients showed a persistent clinical course. Interestingly, PE with or without IVIG/CS was found to be significantly superior to CS and IVIG alone by laboratory tests and the improvement rates in neurological findings were also higher in the former. The retrospective nature of the study as well as the relatively small number of treatments limit the significance of the results, however, laboratory studies such as spinal cord MRI and evoked potentials supplemented the neurological evaluation.

Atopic myelitis frequently presents a chronic persistent course, and the MRI lesions do not change in size over years masquerading as spinal cord tumors [1–3,7,9,10]. Thus, in the present series, immunotherapy was initiated months or years after the onset. Nevertheless, neurological signs and the EDSS scores were improved in three-quarters and one-third of the patients, respectively. Moreover, half the patients showed improvement on either MRI or by EPs. These findings suggest the inflammatory nature of spinal cord lesions, partly reversible by immunotherapy, despite the persistence of small MRI lesions and normal CSF findings [1–3,7]. The notion is consistent with the neuropathological observations indicating chronic active inflammation [9,10].

Concerning the modality of the immunotherapies, PE and PE+IVIG/CS were the most favorable, as determined by neurological examination and laboratory tests, while IVIG was the least effective and CS showed a modest improvement rate as determined by laboratory tests. Although the disease duration at the time of treatment was longer and the EDSS scores were greater in the PE+IVIG/CS group than in the other groups, the treatment was more efficacious than CS and IVIG on laboratory tests.

The high efficacy of PE suggests that humoral factors, possibly driven by Th2 cells, may contribute to sustaining inflammation in the spinal cord. CS treatment was also effective on neurological examination. Its efficacy is similar in other atopic disorders such as bronchial asthma, atopic dermatitis and allergic rhinitis [16–18]; which may be partly attributable to the significant decrease in eosinophils, since they have been shown to infiltrate the spinal cord lesions and their activated products are deposited in the tissues [9,10]. Although the number of trials was small in the IVIG group, its ineffectiveness may suggest that an autoantibody-mediated mechanism does not play a major role in this condition.

Both pathological studies showing eosinophil infiltration and axonal damage from the early course of the disease, and flow cytometric studies on the cytokine balance in peripheral blood lymphocytes showing Th2 dominance in atopic myelitis versus Th1 dominance in MS, indicate that distinct mechanisms are operative between these two conditions [19–22]. In autoimmune diseases affecting the central nervous system (CNS), such as MS, CS has been shown to be effective in an acute phase to reduce the inflammatory response and shorten the exacerbating phase [23]. In contrast, CS appeared to be less effective than PE for atopic myelitis, as shown in the representative case in Fig. 2, further supporting the notion that a distinctive mechanism is operative in this condition. The efficacy of PE appears to be similar to that reported for atypical demyelinating diseases, such as Devic disease [24], in which eosinophils and a Th2-driven mechanism have also been suggested to play roles [25]. PE may be effective for removing activated eosinophil products, such as eosinophil cationic protein (ECP) and major basic protein, which have been shown to be deposited in the spinal cord lesions in atopic myelitis patients [9,10]. Alternatively, removal of cytokines, complements or immune complexes may be relevant.

In summary, our results suggest that immunotherapies, especially those including PE, may be worth trying, even in cases showing a protracted clinical course, long after the onset of myelitis with atopic diathesis. Further studies focusing on cytokines and eosinophil products in the CSF before and after immunotherapy will be required to clarify the mechanism of action.

Acknowledgements

This work was supported in part by a Neuroimmunological Disease Research Committee grant, a Research on Brain Science grant from the Ministry of Health and Welfare, Japan, and Grants 12470142, 12557060 and 12877097 from the Ministry of Education, Science, Sports and Culture, Japan.

References

[1] Kira J, Yamasaki K, Kawano Y, Kobayashi T. Acute myelitis associated with hyperIgEemia and atopic dermatitis. J Neurol Sci 1997;148:199–203.

[2] Kira J, Kawano Y, Yamasaki K, Tobimatsu S. Acute myelitis with hyperIgEaemia and mite antigen specific IgE: atopic myelitis. J Neurol Neurosurg Psychiatry 1998;64:676–9.

[3] Kira J, Kawano Y, Horiuchi I, Yamada T, Imayama S, Furue M, et al. Clinical, immunological and MRI features of myelitis with atopic dermatitis (atopic myelitis). J Neurol Sci 1999;162:56–61.
[4] Horinouchi H, Inobe J, Mori T, Kumamoto T, Tsuda T. A case of atopic myelitis. Rinsho Shinkeigaku 2000;40:218–21.
[5] Furuya T, Miwa H, Hatano T, Miyashita N, Tanaka S, Mizuno Y. Clinical features of myelitis in patients with atopic symptoms. No To Shinkei 2001;53:241–5.
[6] Kuwabara T, Tanaka M. A case of atopic myelitis in the area other than Kyushu Island. Rinsho Shinkeigaku 2001;41:621–4.
[7] Osoegawa M, Ochi H, Minohara M, Murai H, Umehara F, Furuya H, et al. Myelitis with atopic diathesis: a nationwide survey of 79 cases in Japan. J Neurol Sci 2003;209:5–11.
[8] Mosmann TR, Sad S. The expanding universe of T-cell subsets: Th1, Th2 and more. Immunol Today 1996;17:138–46.
[9] Kikuchi H, Osoegawa M, Ochi H, Murai H, Horiuchi I, Takahashi H, et al. Spinal cord lesions of myelitis with hyperIgEemia and mite antigen specific IgE (atopic myelitis) manifest eosinophilic inflammation. J Neurol Sci 2001;183:73–8.
[10] Osoegawa M, Ochi H, Kikuchi H, Shirabe S, Nagashima T, Tsumoto T, et al. Eosinophilic myelitis associated with atopic diathesis: a combined neuroimaging and histopathological study. Acta Neuropathol (Berl) 2003;105:289–95.
[11] Rothe MJ, Grant-Kels JM. Atopic dermatitis: an update. J Am Acad Dermatol 1996;35:1–13 [quiz 4–6].
[12] McDonald WI, Compston A, Edan G, Goodkin D, Hartung HP, Lublin FD, et al. Recommended diagnostic criteria for multiple sclerosis: guidelines from the International Panel on the diagnosis of multiple sclerosis. Ann Neurol 2001;50:121–7.
[13] Kurtzke JF. Rating neurologic impairment in multiple sclerosis: an expanded disability status scale (EDSS). Neurology 1983;33: 1444–52.
[14] Sipe JC, Knobler RL, Braheny SL, Rice GP, Panitch HS, Oldstone MB. A neurologic rating scale (NRS) for use in multiple sclerosis. Neurology 1984;34:1368–72.
[15] Suga R, Tobimatsu S, Kira J, Kato M. Motor and somatosensory evoked potential findings in HTLV-I associated myelopathy. J Neurol Sci 1999;167:102–6.
[16] Rudikoff D, Lebwohl M. Atopic dermatitis. Lancet 1998;351: 1715–21.
[17] Nielsen LP, Dahl R. Comparison of intranasal corticosteroids and antihistamines in allergic rhinitis: a review of randomized, controlled trials. Am J Respir Medicine 2003;2:55–65.
[18] Leone FT, Fish JE, Szefler SJ, West SL. Systematic review of the evidence regarding potential complications of inhaled corticosteroid use in asthma: collaboration of American College of Chest Physicians, American Academy of Allergy, Asthma, and Immunology, and American College of Allergy, Asthma, and Immunology. Chest 2003;124:2329–40.
[19] Horiuchi I, Kawano Y, Yamasaki K, Minohara M, Furue M, Taniwaki T, et al. Th1 dominance in HAM/TSP and the optico-spinal form of multiple sclerosis versus Th2 dominance in mite antigen-specific IgE myelitis. J Neurol Sci 2000;172:17–24.
[20] Wu XM, Osoegawa M, Yamasaki K, Kawano Y, Ochi H, Horiuchi I, et al. Flow cytometric differentiation of Asian and Western types of multiple sclerosis, HTLV-1-associated myelopathy/tropical spastic paraparesis (HAM/TSP) and hyperIgEaemic myelitis by analyses of memory CD4 positive T cell subsets and NK cell subsets. J Neurol Sci 2000;177:24–31.
[21] Ochi H, Wu XM, Osoegawa M, Horiuchi I, Minohara M, Murai H, et al. Tc1/Tc2 and Th1/Th2 balance in Asian and Western types of multiple sclerosis, HTLV-I-associated myelopathy/tropical spastic paraparesis and hyperIgEaemic myelitis. J Neuroimmunol 2001; 119:297–305.
[22] Ochi H, Osoegawa M, Murai H, Minohara M, Taniwaki T, Kira J. Presence of IgE antibodies to bacterial superantigens and increased IL-13-producing T cells in myelitic patients with atopic diathesis. Int Arch Allergy Immunol 2004;134:41–8.
[23] Durelli L, Cocito D, Riccio A, Barile C, Bergamasco B, Baggio GF, et al. High-dose intravenous methylprednisolone in the treatment of multiple sclerosis: clinical-immunologic correlations. Neurology 1986;36:238–43.
[24] Weinshenker BG, O'Brien PC, Petterson TM, Noseworthy JH, Lucchinetti CF, Dodick DW, et al. A randomized trial of plasma exchange in acute central nervous system inflammatory demyelinating disease. Ann Neurol 1999;46:878–86.
[25] Lucchinetti CF, Mandler RN, McGavern D, Bruck W, Gleich G, Ransohoff RM, et al. A role for humoral mechanisms in the pathogenesis of Devic's neuromyelitis optica. Brain 2002;125: 1450–61.

INFECTION AND IMMUNITY, June 2004, p. 3592–3603 Vol. 72, No. 6
0019-9567/04/$08.00+0 DOI: 10.1128/IAI.72.6.3592–3603.2004

Legionella dumoffii DjlA, a Member of the DnaJ Family, Is Required for Intracellular Growth

Hiroko Ohnishi,[1,2] Yoshimitsu Mizunoe,[1]* Akemi Takade,[1] Yoshitaka Tanaka,[3] Hiroshi Miyamoto,[4] Mine Harada,[2] and Shin-ichi Yoshida[1]

Department of Bacteriology[1] and Department of Medicine and Biosystemic Science, Internal Medicine,[2] Faculty of Medical Sciences, and Division of Pharmaceutical Cell Biology, Graduate School of Pharmaceutical Sciences,[3] Kyushu University, Fukuoka 812-8582, and Department of Microbiology, School of Medicine, University of Occupational and Environmental Health, Kitakyushu 807-8555,[4] Japan

Received 12 November 2003/Returned for modification 5 January 2004/Accepted 10 February 2004

***Legionella dumoffii* is one of the common causes of Legionnaires' disease and is capable of replicating in macrophages. To understand the mechanism of survival within macrophages, transposon mutagenesis was employed to isolate the genes necessary for intracellular growth. We identified four defective mutants after screening 790 transposon insertion mutants. Two transposon insertions were in genes homologous to *icmB* or *dotC*, within *dot/icm* loci, required for intracellular multiplication of *L. pneumophila*. The third was in a gene whose product is homologous to the 17-kDa antigen forming part of the VirB/VirD4 type IV secretion system of *Bartonella henselae*. The fourth was in the *djlA* (for "*dnaj*-like *A*") gene. DjlA is a member of the DnaJ/Hsp40 family. Transcomplementation of the *djlA* mutant restored the parental phenotype in J774 macrophages, A549 human alveolar epithelial cells, and the amoeba *Acanthamoeba culbertsoni*. Using confocal laser-scanning microscopy and transmission electron microscopy, we revealed that in contrast to the wild-type strain, *L. dumoffii djlA* mutant-containing phagosomes were unable to inhibit phagosome-lysosome fusion. Transmission electron microscopy also showed that in contrast to the virulent parental strain, the *djlA* mutant was not able to recruit host cell rough endoplasmic reticulum. Furthermore, the stationary-phase *L. dumoffii djlA* mutants were more susceptible to H_2O_2, high osmolarity, high temperature, and low pH than was their parental strain. These results indicate that DjlA is required for intracellular growth and organelle trafficking, as well as bacterial resistance to environmental stress. This is the first report demonstrating that a single DjlA-deficient mutant exhibits a distinct phenotype.**

Legionella dumoffii was first isolated from cooling-tower water in 1979 (18) and later from a postmortem lung specimen in the same year (40) as an atypical *Legionella*-like organism. It was later classified by Brenner (11) as a new species, *L. dumoffii*. *Legionella* species are gram-negative, facultative intracellular parasites of freshwater amoebae in nature and are capable of growing within alveolar macrophages and epithelial cells after being accidentally transmitted to humans (22). The most common human pathogen in the genus *Legionella* is *L. pneumophila*, the causative agent of Legionnaires' disease (71). Humans contract the disease from contaminated environmental sources, primarily by aspiration of aerosolized water sources (22). After internalization by alveolar macrophages, *L. pneumophila*-containing phagosomes do not acidify (34) or fuse with lysosomes (33). Instead, the mitochondria, smooth vesicles, and rough endoplasmic reticula (RER) near these *L. pneumophila*-containing vacuoles are recruited, and *L. pneumophila* begins to multiply in this unique niche (32). This altered endocytic pathway is considered to be controlled by the Dot/Icm type IV protein secretion system (5, 17, 48, 55, 56, 74). The *dot/icm* genes are essential for the intracellular growth of *L. pneumophila* (5, 51, 60). The presence of the *dot/icm* loci in several species of *Legionella* was shown by Southern or PCR analysis (4, 36, 43); however, the contributions of these loci to the pathogenesis of other species have yet to be investigated.

L. dumoffii is the fourth or fifth most common pathogen causing Legionnaires' disease (8, 71). Some of proteins or factors which may promote *L. pneumophila* pathogenesis, such as flagella, catalase, and gelatinase, are also present in *L. dumoffii*. Several putative virulence factors—lipase, oxidase, and a zinc metalloprotease—are absent in *L. dumoffii* (6, 11, 52). *L. dumoffii* is capable of infecting and replicating within Vero cells and the human lung alveolar epithelial cell line A549 in vitro (41, 42). To elucidate the molecular mechanisms of the intracellular growth of this organism, we attempted to isolate the mutants that exhibited defective growth phenotypes in J774 mouse macrophage-like cells and A549 human type II alveolar epithelial cells by using transposon mutagenesis. We isolated four clones attenuated in virulence within mammalian cells by screening 790 derivatives with Tn*903*dII*lacZ* insertions. Two of four genes flanking the transposon insertions encode the proteins homologous to *L. pneumophila* IcmB and DotC (5, 51, 60), respectively. One gene has similarity to *virB5* (17-kDa antigen) in the VirB/VirD4 type IV secretion system of *Bartonella henselae* (14, 49, 59). The deduced protein encoded by a fourth gene showed homology to DjlA proteins (16). The DjlA homologue, a member of the DnaJ/Hsp40 family, was originally identified in *Escherichia coli* as a product of a hypothetical open reading frame (13, 72), and since then homologues have been identified in many other bacterial species, such as *Coxiella burnetti* (73), *Salmonella enterica* serovar Ty-

* Corresponding author. Mailing address: Department of Bacteriology, Faculty of Medical Sciences, Kyushu University, Fukuoka 812-8582, Japan. Phone: 81-92-642-6128. Fax: 81-92-642-6133. E-mail: ymizunoe@bact.med.kyushu-u.ac.jp.

TABLE 1. Bacterial strains and plasmids used in this study

Strain or plasmid	Relevant characteristics	Source or reference
Strains		
E. coli		
DH5α	F⁻*endA1 hsdR17 supE44D thi-1 recA1*Δ(*argF-lacZYA*)*U169*(ϕ80δ *lacZM15*) *gyrA96*λ⁻	30
VCS257	DP50 *sup* F[*supE44 supF58 hsd53*(r_B m_B) *dapD8 lacY1 gln*V44 Δ(*gal-uvrB*)47 *tyrT58 gyrA29 tonA53* Δ(*thyA57*)]	Stratagene
L. dumoffii Tex-KL		ATCC 33343
HOLD254	Tex-KL *djlA*::Tn*903*dII*lacZ*	This study
HOLD491	Tex-KL *icmB(dotO)*::Tn*903*dII*lacZ*	This study
HMLD4001	Tex-KL 17-kDa antigen::Tn*903*dII*lacZ*	This study
HMLD4002	Tex-KL *dotC*::Tn*903*dII*lacZ*	This study
HOLD254-1	Tex-KL *djlA*::Tn*903*dII*lacZ*/pHRO18	This study
HOLD254-2	Tex-KL *djlA*::Tn*903*dII*lacZ*/pHRO25	This study
Plasmids		
pGEM-T Easy	Amp^r, *lacZ*, general cloning vector	Promega
pUC19	Amp^r, parental cloning vector	70
pBR322	*ori*R (ColE1); Amp^r Tc^r	New England Biolabs
pHC79	Wide-host-range pBR322 origin cosmid vector; Amp^r Tc^r	31
pLAW317	*rpsL* MCS[a] *oriT*(RK2) Cm^r*loxP ori*R(ColE1) Amp^r*loxP*	68
pLAW330	pLAW317::Tn*903*dII*lacZ tnpA*(Tn*903*) *oriR*(f1)	68
pMMB207	RSF1010 derivative, *lncQ lac I*^{q} Cm^r P*tac oriT*	47
pMMB207c	pMMB207 with 8-bp insertion in *mobA*; Mob	45
pHRO1	Tn*903*dII*lacZ*-containing HindIII fragment from HOLD254 in pBR322	This study
pHRO2	Tn*903*dII*lacZ*-containing BamHI fragment from HOLD491 in pBR322	This study
pHRO3	Tn*903*dII*lacZ*-containing HindIII fragment from HMLD4001 in pBR322	This study
pHRO4	Tn*903*dII*lacZ*-containing HindIII fragment from HMLD4002 in pBR322	This study
pHRO17	Amp^r; 4-kbp ScaI-EcoRI fragment containing *djlA* gene in pUC19	This study
pHRO18	4-kbp Pst-EcoRI fragment containing *djlA* from pHRO17 in pMMB207c	This study
pHRO24	PCR fragment of *djlA* cloned into pGEM-T Easy vector	This study
pHRO25	EcoRI-PstI fragment (1,155 bp) containing *djlA* from pHRO24 cloned into pMMB207c	This study

[a] MCS, multiple-cloning site.

phimurium, *Klebsiella pneumoniae*, and *Vibrio cholerae*. DjlA carries the J-domain characteristic of the DnaJ/Hsp40 family and is essential for interaction with the Hsp70 homologue, DnaK, by increasing its ATPase activity (67). Overproduction of DjlA stimulates colanic acid production in *E. coli* (15, 16, 27, 73). Analysis of the DjlA null mutant demonstrated that the gene was not essential for viability (16). Although DjlA homologue is present in *L. pneumophila* (10), the role of this gene in pathogenesis has yet to be determined.

In this study, we investigated the role of the *djlA* gene in avoidance of fusion with lysosomes and its role in organelle trafficking within macrophages and in bacterial resistance to environmental stresses such as oxidative products, high temperature, high salt concentrations, and acidic pH.

MATERIALS AND METHODS

Bacterial Strains, plasmids, and media. The bacterial strains and plasmids used in this work are described in Tables 1 and 2. The *L. dumoffii* Tex-KL strain and its derivatives were grown on buffered charcoal-yeast extract (BCYE) agar plates or in buffered yeast extract (BYE) broth. BYE broth was based on the formation of BCYE, but the charcoal and agar were omitted. *E. coli* DH5α (Toyobo Co., Ltd., Osaka, Japan) was used for the majority of the cloning experiments. As required, antibiotics were used at the following concentrations: kanamycin (KM), 30 μg/ml; chloramphenicol (CM), 5 or 20 μg/ml (for *L. dumoffii*); KM, 30 μg/ml; ampicillin (AMP), 50 μg/ml; CM, 20 μg/ml (for *E. coli*).

Cell culture. J774A.1 macrophages (JCRB9108), refered to as J774 in this paper, were derived from mouse macrophage-like cells. The cell line A549 (JCRB0076) was donated by the Health Science Research Resources Bank, Osaka, Japan. The cells were established from a human alveolar epithelial carcinoma and have characteristics of well-differentiated type II pneumocytes. J774 cells and A549 cells were cultured in RPMI 1640 medium (GIBCO, Grand Island, N.Y.) supplemented with 10% fetal bovine serum (FBS; Dainippon

TABLE 2. Strains of *Legionella* species used and their clinical relevance

Legionella strain	Source	Clinical relevance
L. pneumophila serogroup1 (ATCC 33153)	Human	Yes
L. pneumophila serogroup6 (ATCC 33215)	Human	Yes
L. dumoffii (ATCC 33343)	Human	Yes
L. longbeachae (ATCC 33462)	Human	Yes
L. micdadei (ATCC 33218)	Human	Yes
L. bozemanii (ATCC 33217)	Human	Yes
L. feelei (ATCC 35849)	Human	Yes
L. gormanii (ATCC 33297)	Soil	Yes
L. jordanis (ATCC 33623)	Water	Yes
L. quinlivanii (ATCC 43830)	Water	No
L. moravica (ATCC 43877)	Water	No
L. gratiana (ATCC 49413)	Water	No
L. geestiana (ATCC 49504)	Water	No
L. rubrilucens (ATCC 35304)	Water	No
L. worsleiensis (ATCC 49508)	Water	No
L. jamestowniensis (ATCC 35298)	Soil	No
L. adelaidensis (ATCC 49625)	Water	No

Pharmaceutical, Osaka, Japan). *Acanthamoeba culbertsoni* (44) was propagated at 28°C in 25-cm^2 flasks (Falcon) containing 8 ml of peptone yeast extract glucose (PYG) and AC buffer (PYG + AC) (9, 46).

DNA manipulation. Restriction enzymes and T4 DNA polymerase were purchased from Takara Shuzo Co., Ltd. (Kyoto, Japan) and Toyobo Co., Ltd. (Osaka, Japan). Calf intestine alkaline phosphatase was purchased from New England Biolabs Inc. (Beverly, Mass.). PCR amplification was performed by using The Ready To Go PCR-Beads (Amersham Pharmacia Biotech, Piscataway, N.J.) or Ex-Taq polymerase (Takara, Kyoto, Japan). Oligonucleotides used for PCR amplification were purchased from Japan Flour Co., Ltd. (Tokyo, Japan). Plasmid DNA was isolated from *E. coli* and *L. dumoffii* by using the Wizard Plus Mini Prep (Promega, Madison, Wis.) or the alkaline lysis method (58). Chromosomal DNA of *L. dumoffii* was purified using the Genomic Prep cells and tissue DNA isolation kit (Amersham Pharmacia Biotech). Electroporations were performed with a Bio-Rad Gene Pulser, as recommended by the manufacturer. Purification of DNA fragments from agarose gels for subcloning or labeling was carried out with a GFX PCR DNA and gel band purification kit (Amersham Pharmacia Biotech).

Transposon mutagenesis and construction of a bank of mutants. *L. dumoffii* was mutated with the Tn*903* derivative Tn*903*dII*lacZ*, as described previously (68). Tn*903*dII*lacZ* confers KM resistance (Km^r) and contains a 5′-truncated *lacZ* gene. Briefly, after electroporation of plasmid pLAW330, containing Tn*903*dII*lacZ*, into *L. dumoffii* Tex-KL, bacteria were incubated in BYE broth for 5 h at 37°C and plated onto BCYE-KM plates. Km^r transformants containing β-galactosidase activity were identified as blue colonies after the the plates were overlaid with 0.8% agar containing 0.6 mg of 5-bromo-4-chloro-3-indolyl-β-D-galactoside (X-Gal) per ml. Km^r Cm^s colonies were saved as simple Tn*903*dII*lacZ* insertion mutants of *L. dumoffii*.

Southern hybridization. Chromosomal DNA from *L. dumoffii* strains was digested with HindIII, resolved on a 0.7% agarose gel in TBE buffer, and blotted onto a nylon membrane. DNA probes were prepared by random-primed labeling with digoxigenin-1 1-dUTP. The methods for prehybridization and hybridization and the washing conditions were the same as described previously (58), and the procedure for colorimetric detection of hybridized DNA was performed using the digoxigenin system (Roche Diagnostic Co., Indianapolis, Ind.).

Cloning and sequencing of the chromosomal junction of Tn*903*dII*lacZ* insertion in the mutants. Genomic DNA from the *L. dumoffii* mutants was digested with HindIII or BamHI and ligated to HindIII- or BamHI-digested pBR322. The ligation was used to transform DH5α, and the transformation mixture was plated on Luria-Bertani agar plates containing KM and AMP. Plasmid DNA was extracted, and the regions flanking Tn*903*dII*lacZ* were sequenced with the *lacZ* primer (5′-CCCAGTCACGACGTTG-3′) and the Km^r primer (5′-AATTTAA TCGCGGCCTCGAG-3′), corresponding to the 5′ and 3′ ends, respectively, of Tn*903*dII*lacZ*.

Construction of plasmids for complementation. For wild-type *L. dumoffii* genomic library construction, the genomic DNA was isolated from *L. dumoffii* and partially digested with Sau3 AI, and fragments of about 40 kb were purified. The fragments were ligated to the BamHI-digested, calf intestinal alkaline phosphatase-treated cosmid vecter pHC79 (31). The ligation products were packaged, in vitro, using the GigapackII Gold packaging system (Stratagene). Packaged hybrid cosmids were then used to infect *E. coli* strain *VCS*257. Recombinant clones were screened for the presence of a 1,085-bp PCR product (254-45), amplified using primers 254-4 (5′-GCTTCTTCCTTTCCACCATAA-3′) and 254-5 (5′-AGGTAGGCCTTGGGCAATTA-3′), by colony hybridization techniques. The probes used for colony hybridization were labeled with the digoxigienin random-primed DNA-labeling system (Roche). About 1,000 recombinant clones from the library were plated on the Luria-Bertani–plus-AMP plates for screening. Several positive cosmid clones were identified. The 4-kb ScaI-EcoRI fragment containing 254-45 from one of these cosmid clones was cloned into HincII-EcoRI-digested pUC19 to generate pHRO17. The recombinant clone was confirmed to contain 254-45 by Southern blot hybridization. The 4-kb PstI-EcoRI fragment from pHRO17 was cloned into shuttle vecter pMMB207c digested with PstI and EcoRI to generate pHRO18. pMMB207c is a nonmobilizable derivative of pMMB207 containing an 8-bp insertion within the *mobA* gene (at base 3325) and replicates stably in *Legionella* spp. (45). pHRO18 was electroporated into HOLD254 to yield the complemented strain HOLD254-1. The DNA fragment containing the *djlA* gene was PCR amplified from plasmid pHRO17 by using primer pair djlA-1-EcoRI (5′-GGGAATTCGAGTAGATA CGAAGCAGGGT-3′) and djlA-2-PstI (5′-GGCTGCAGTTCCACCATAAAC GGACTACA-3′). EcoRI and PstI sites (underlined sequences) were incorporated into these primers, respectively. The 1,155-bp PCR product that was generated contained 158 bp upstream of the ATG codon of *djlA* and 72 bp downstream of the stop codon of *djlA*. This PCR product was ligated into the pGEM-T Easy vector (Promega), resulting in pHRO24. The 1,155-bp EcoRI-PstI fragment from pHRO24 was then cloned into EcoRI-PstI-digested pMMB207c, creating pHRO25. The *djlA* mutant of *L. dumoffii*, HOLD254, was transformed with pHRO25 by electroporation. One of the transformants containing the desired plasmid was designated HOLD254-2. The cloned *djlA* gene was sequenced by using the primer within pMMB207c (pMMB207c-1; 5′-GTG TGGAATTGTGAGCGGAT-3′) and the primer within the *djlA* gene (254-3; 5′-GCTGATGGGCTGGATAGCAA-3′).

DNA sequence analysis of the region surrounding the *djlA* gene. Primer pair djlA-3 (5′-AAGGATGGTAACTCTGACTCT-3′) and pHC79-2 (5′-TTGGAG CCACTATCGACTAC-3′) within the *djlA* gene and pHC79, respectively, were used to amplify the flanking region of the *djlA* gene from the cosmid clone containing *djlA* gene. This 4-kb PCR product and the 4-kb plasmid DNA within pHRO17 were sequenced using a primer walking technique. DNA-sequencing reactions were performed on plasmid templates with the CEQ DTCS-Quick Start kit (Beckman Coulter, Inc., Fullerton, Calif.) and the CEQ DNA analysis system (Beckman Coulter, Inc.). The nucleotide sequences and deduced amino acid sequences were compared to the GenBank database by using the programs BLASTX and BLASTP and also to the incomplete genomic database of *L. pneumophila* Philadelphia I (http://genome3.cpmc.columbia.edu/~legion/ngnp1033033). Motif searches were carried out using the Prosite program.

Intracellular growth assay. Growth of *L. dumoffii* in J774 cells and A549 cells was determined by using a previously described standard intracellular growth assay (43, 74). *L. dumoffii* strains were grown in BYE broth to the early stationary phase. Approximately 2×10^9 bacteria were pelleted, resuspended, and diluted (1:1,000) in RPMI 1640 tissue culture medium. The bacteria were then added to J774 cells and A549 cells (2×10^5 per well) in 24-well dishes to give a multiplicity of infection (MOI) of about 10. The infected cells were incubated at 37°C under 5% CO_2–air for 1.5 h and washed three times with phosphate-buffered saline (PBS) to remove extracellular bacteria. To measure bacterial internalization, 1 ml of sterile distilled H_2O was added to the wells to release intracellular bacteria from the host cells, and CFU were determined by plating dilutions on BCYE agar plates. To each of the remaining wells, 0.5 ml of fresh tissue culture medium was added. At 24-h intervals, the intracellular and extracellular bacteria in each well were combined, and the total CFU was determined by plating the dilutions onto BCYE agar plates. Infection of *A. culbertsoni* was carried out in an almost identical manner, except that bacteria were suspended in AC buffer and 0.05% Triton X-100 was added to release intracellular bacteria.

Assessment of phagosome-lysosome fusion by confocal microscopy. *L. dumoffii* strains were grown overnight to saturation at 37°C in BYE broth. They were added at an MOI of 25 to 50 to 8×10^4 J774 cells on glass coverslips in 24-well tissue culture plates. The plates were centrifuged at $150 \times g$ for 5 min at room temperature and incubated for 20 min in 5% CO_2–air at 37°C. Extracellular bacteria were removed by washing three times with PBS, and fresh tissue culture medium was added to each well. The plates were returned to the incubator for 4 h. Cells were fixed for 15 min at room temperature in P-PFA (4% paraformaldehyde in 1 × PBS [pH 7.4]) (43, 74). Coverslips were immersed in PBS–0.1% Saponin for 5 min to permeabilize the cells and blocked with 5% FBS in PBS for 5 min. Lysosomes and late endosomes were stained with rat monoclonal antibody 1 D4B (1:100) specific for LAMP-1 or Ab1 93 (1:100) specific for LAMP-2, and the bacteria were stained with rabbit anti-*L. dumoffii* polyclonal antibody (1: 10,000) for 1 h. The cells were washed with blocking solution three times and incubated for 30 min with Cy3-labeled goat anti-rat secondary antibody (1:300) and Alexa488-labeled goat anti-rabbit secondary antibody (1:300). The coverslips were then washed three times with blocking solution. All antibody dilutions were performed with PBS containing 0.5% FBS and 0.1% Saponin. Coverslips were inverted onto 1 μl of mounting medium (50% glycerol) on glass slides (39). Fluorescence was viewed using a Radiance 2100 MP confocal microscope (Bio-Rad Laboratories, Richmond, Calif.). Alexa488- and Cy3-labeled secondary antibodies were purchased from Molecular Probes (Eugene, Oreg.). Rat monoclonal antibodies to LGP107 (mouse LAMP-1) and LGP96 (mouse LAMP-2) were purified from mouse liver lysosomal membranes, as described previously (23).

Quantification of phagosome-lysosome fusion by electron microscopy. To label cell lysosomes, J774 macrophages were incubated with bovine serum albumin (BSA)-conjugated colloidal 15-nm-diameter gold particles (BSA-gold) overnight, chased for 3 h, and pulsed with stationary-phase *L. dumoffii* strains at an MOI of 50 (19, 33). At 4 h postinfection, the cells were fixed and processed for electron microscopy as previously described (66). Briefly, infected macrophages were fixed with 2% glutaraldehyde and then with 1% OsO_4, dehydrated with ethanol, and embedded in Epon. Ultrathin sections were stained with uranyl

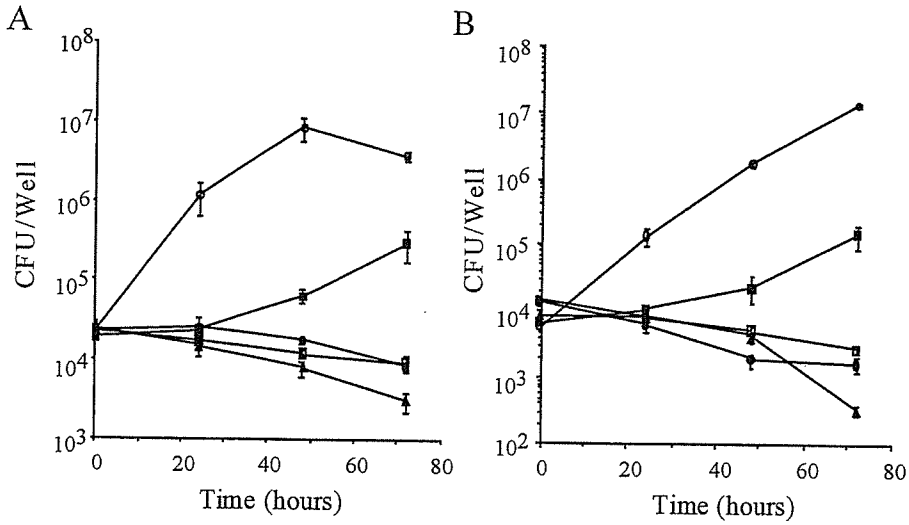

FIG. 1. Intracellular growth of *L. dumoffii* strains within J774 mouse macrophages (A) and A549 human epithelial cells (B). The formation of colonies (CFU per milliliter) was determined at the times indicated, in triplicate, for at least two independent experiments. Error bars indicate the standard deviations determined from samples taken from one experiment. Symbols: ○, *L. dumoffii* wild-type strain; ■, HOLD254; □, HOLD491; ●, HMLD4001; △, HMLD4002.

acetate followed by lead citrate and examined by electron microscopy in a JEM 2000EX instrument (JEOL, Ltd., Tokyo, Japan).

Examination of RER recruitment by transmission electron microscopy. J774 cells were plated in 90-mm-diameter petri dishes (2×10^5 cells/ml) and infected with stationary-phase *L. dumoffii* strains at an MOI of 20 for 8 and 24 h (32). Ultrathin sections were prepared as described above.

Assays for survival under stress conditions. *L. dumoffii* strains were grown for 2 to 3 days on BCYE agar plates and used to inoculate 4 ml of BYE medium. The bacteria were then grown at 37°C with aeration for at least 16 h. The initial CFU count was about 10^{10} per ml. Cells were divided into aliquots, centrifuged, and resuspended in equal volumes of 1 × M63 salts [22.0 mM KH_2PO_4, 40.2 mM K_2HPO_4, 14.6 mM $(NH_4)_2SO_4$ 500 nM $FeSO_4$ (pH6.5)]. One aliquot was used for measuring the untreated CFU. For heat shock, aliquots were transferred to 48°C and incubated for 60 min. For oxidative stress, aliquots were exposed to 10 mM H_2O_2 for 30 min. For osmotic shock, aliquots were exposed to 5 M sodium chloride for 30 min. For acid shock, aliquots were resuspended in 0.1 M citric acid (pH 3) for 5 min. Except for heat stress, the cells were incubated in a 37°C heat block. At the indicated time points, the cells were washed with 1 × M63 salts and serially diluted to determine the CFU on BCYE agar plates (29).

Detection of a *djlA* gene in other *Legionella* spp. The presence of *djlA* in 17 different strains of *Legionella* spp. was examined by PCR with the primer pair djlA-cons-1 (5′-ATAACAACCTGGTGGGGAAA-3′) and djlA-cons-2 (5′-TG GGCAATTAATTTATCTGGATG-3′), located in the transmembrane domain (TMD) and J domain within the *djlA* gene, respectively, which gave a 791-bp product. PCR was carried out by using chromosomal DNA from BCYE plate-grown bacteria as a template.

RESULTS

Isolation of intracellular growth mutants. Wild-type *L. dumoffii* Tex-KL was mutagenized with Tn*903*dIII*lacZ* as described previously (57, 68). Plasmid pLAW330 containing Tn*903*dIII*lacZ* was introduced into *L. dumoffii*, and 790 Km^r Cm^s mutants of *L. dumoffii* (HOLD strains 1 to 656 and HMLD strains 4004 to 4044 and 4048 to 4140) with various levels of β-galactosidase activity were isolated. The 790 mutants were individually screened for their ability to kill mouse macrophage-like J774 cells and human alveolar epithelial A549 cells. The mutants were grown for 2 days in 96-well tissue culture plates containing BYE medium. Then 5-μl samples of 2-day-old cultures of mutants were transferred to another 96-well tissue culture plate containing J774 cells or A549 cells. At each 24-h time point after infection, the monolayers were visually examined to determine the extent of killing of both J774 cells and A549 cells. From several assays, we isolated five mutants, based on their reproducible phenotypes. Southern blot analysis of the HindIII-digested genomic DNA of each of the five mutants probed with pLAW330 showed that four of them contained a single copy of the Tn*903*dIII*lacZ* insertion and that these insertions were distributed in distinct locations within the chromosome of *L. dumoffii* (data not shown). For reasons not yet understood, one of the mutants showed no hybridization. Therefore, the four strains were chosen for further analysis. In vitro, the growth of these four mutants in BYE broth and on BCYE agar plates was similar to that of the wild-type strain (data not shown).

Intracellular growth phenotype of the mutants within J774 macrophages and alveolar epithelial cells. We examined the four candidates for their capacity to survive and to replicate within J774 macrophages and A549 epithelial cells. Bacterial CFU were determined over 3 days. The wild-type strain multiplied over 100-fold during the 3-day incubation period within J774 macrophages (Fig. 1A). HOLD254 showed a 1-log-unit increase after 3 days of incubation, whereas HOLD491, HMLD4001, and HMLD4002 did not grow during the incubation period in J774 cells. Within A549 epithelial cells (Fig. 1B), the wild-type strain increased approximately 1,000-fold over the 3-day period, while there was a 10-fold increase in the number of intracellular bacteria of HOLD254 over 3 days. For HOLD491 and HMLD4001, the number of CFU after 3 days of infection decreased 1 log unit to the initial number of CFU, and HMLD4002 was severely defective in intracellular survival (Fig. 1B).

Sequence analysis of the junctions of Tn*903*dIII*lacZ* insertions. We cloned the HindIII fragment containing the Tn*903*dIII*lacZ* insert and the flanking sequences of the mutants (HOLD254, HOLD491, HMLD4001, and HMLD4002). Using

TABLE 3. Sequence similarities of *L. dumoffii* genes responsible for intracellular multiplication[a]

Mutant strain	Homologous gene	Organism	% Identity	% Positive
HOLD254	*djlA*	*Legionella pneumophila*	61	73
HOLD491	*icmB/dotO*	*Legionella pneumophila*	89	95
HMLD4001	17-kDa antigen gene	*Bartonella henselae*	26	43
HMLD4002	*dotC*	*Legionella pneumophila*	85	92

[a] The values are taken from a Basic Local Alignment Search Tool for amino acid comparison (BLASTX program).

the primer within Tn*903*dII*lacZ*, we partially sequenced and analyzed them to identify the genes responsible for intracellular multiplication. The results are summarized in Table 3. Sequence homology searches against the Gen Bank database were done with these genes and corresponding proteins. HOLD254, HOLD491, and HMLD4002 contain insertions within the genes homologous to known *L. pneumophila* genes. The gene disrupted in HOLD254 is the *djlA* (for "*dnaJ*-like *A*") gene, encoding a member of the Hsp40 protein family, which has not been characterized in *L. pneumophila*. HOLD491 and HMLD4002 had a transposon insertion in their sequences similar to *icmB (dotO)* and *dotC*, respectively, identified as genes essential for intracellular growth in *L. pneumophila* (5, 51). HMLD4001 had an insertion within a gene whose product showed amino acid similarity to the 17-kDa antigen, VirB5, of *B. henselae*; the gene is located within the *virB* locus, which encodes a putative type IV secretion system together with the downstream *virD4* gene (14, 49, 59). Recently, Schulein and Dehio (59) also showed that VirB4 and VirD4, encoded by the *virB* and *virD4* loci of *B. tribucorum*, were required for establishing intraerythrocytic bacteremia.

Complementation of an *L. dumoffii djlA* mutant. DjlA is known to be a heat shock protein DnaJ/Hsp40 homologue. The virulence of the *djlA* mutant was compared with that of the wild-type strain and the *djlA*-complemented mutant in J774 macrophages, A549 epithelial cells, and *A. culbertsoni*. The *djlA* mutant showed only a 100-fold increase in intracellular replication within *A. culbertsoni* (Fig. 2C). As shown in Fig. 2, bacterial growth was fully restored in the complemented strains HOLD254-1 and HOLD254-2. The restoration of the wild-type-level of multiplication of the *djlA* mutant within these cells, achieved after complementation in *trans* with the cloned *djlA* gene, is proof of the important role of *djlA* in the intracellular growth of *L. dumoffii*.

Complete sequence and genetic structure of *djlA*. Figure 3A shows the organization around the *djlA* gene and the location of the Tn*903*dII*lacZ* insertion. The transposon insertion (Tn) was located in the J domain at the C terminus of the predicted protein, which was the defined feature of the DnaJ family of molecular chaperones (16, 27). Since the two genes (*waaA* and *orf1*) which flanked *djlA* were both oriented in the opposite direction from the *djlA*, we consider the *djlA* to be transcribed

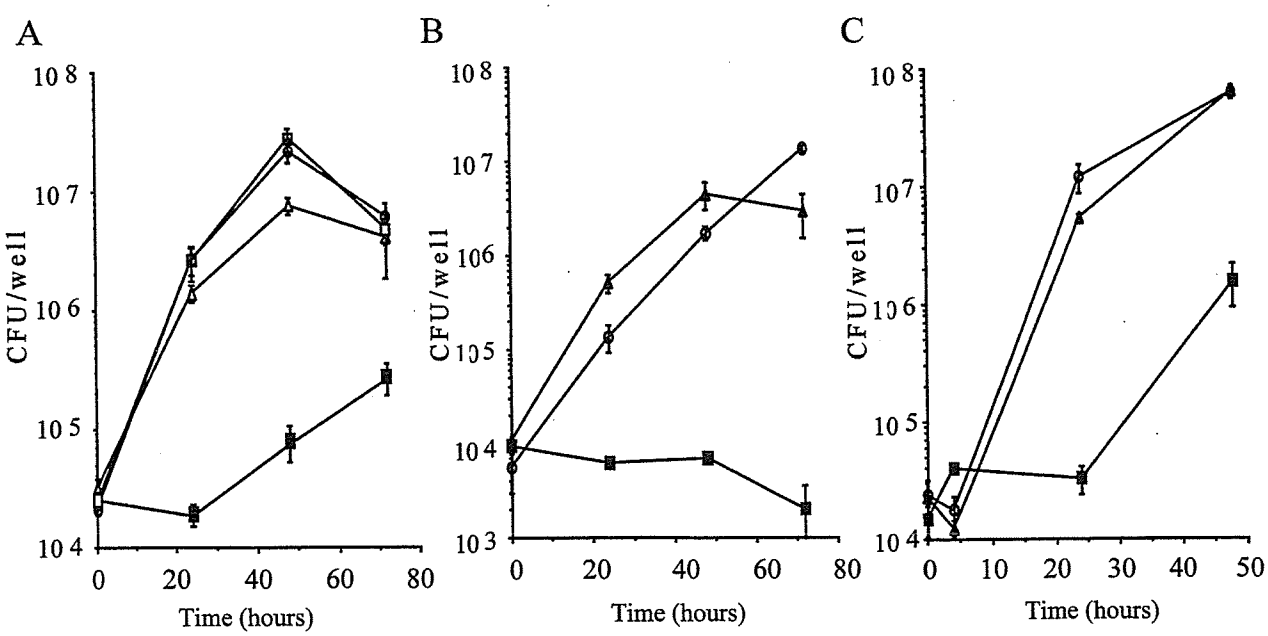

FIG. 2. Complementation of intracellular growth defects of *djlA* mutant HOLD254 in J774 macrophages (A), in A549 epithelial cells (B), and in *A. culbertsoni* (C). Growth was measured over 72 h (A and B) or 48 h (C). The data points and error bars represent the mean CFU/well for triplicate samples from a typical experiment (performed at least twice) and their standard deviations. Symbols: ○, *L. dumoffii* wild-type strain; ■, HOLD254; △, HOLD254-1 (*djlA*/pHRO18); □, HOLD254-2 (*djlA*/pHRO25).

monocistronically, and this transposon has no polar effect. The deduced amino acid sequence of *L. dumoffii* DjlA, together with *L. pneumophila* DjlA and *E. coli* DjlA, is presented in Fig. 3B. The putative *L. dumoffii djlA* gene encodes a protein of 302 amino acids with a predicted molecular mass of 35.33 kDa and an isoelectric point of 9.65. The protein size is similar to that of the *L. pneumophila* (296 amino acids) and *E. coli* (271 amino acids) proteins. *L. dumoffii* DjlA has 61% identity to *L. pneumophila* DjlA and 32% identity to *E. coli* DjlA (10, 16, 73). A potential TMD at the N terminus contains six glycines, spaced through the TMD at every three to five residues, which is similar to the structure of the TMD of *E. coli* (15, 16). There is a remarkable difference in the N terminus of DjlA protein between *E. coli* and *Legionella* spp. Clarke et al. (16) have demonstrated that *E. coli* DjlA is localized to the inner membrane and has a rare type III topology (i.e. N-out, C-in), with the N-terminal 6 to 8 residues located in the periplasm. *Legionella* spp. have longer stretches (15 residues) before the TMD structure, which are probably exposed in the periplasm. Another unique feature of *Legionella* DjlA is a glutamate-serine (QS)-rich spacer located before the J domain, instead of the glutamate-glycine (QG)-rich spacer of *E. coli* DjlA (Fig. 3B) (16). The cellular role of these QS- or QG-rich regions remain to be elucidated.

Quantification of endocytic maturation. To determine whether the *L. dumoffii* strains were able to inhibit endocytic maturation, we measured the colocalization of *L. dumoffii* phagosomes with endocytic markers LAMP-1 and LAMP-2. J774 macrophages were infected with postexponential phase *L. dumoffii* strains for 4 h (Fig. 4). The permeabilized cells were stained with monoclonal antibody 1D4B or Abl 93, specific for late endosomal and lysosomal proteins, LAMP-1 or LAMP-2. The *djlA* mutant was found in phagosomes that contained LAMP-1 (Fig. 4A), indicating that these vacuoles had fused with late endosomes, whereas, phagosomes containing wild-type *L. dumoffii* did not colocalize with LAMP-1 (Fig. 4A). When each *L. dumoffii* strain found in the phagosomes was scored for fusion with the late endosomal/lysosomal markers LAMP-1 and LAMP-2, approximately 80% of the wild-type bacteria were found in LAMP-1- and LAMP-2-negative phagosomes while 50 to 60% of the HOLD254 was found in LAMP-1- and LAMP-2-positive compartments (Fig. 4B). We also performed the same analysis for HOLD4002, the *dotC* mutant, and found that this mutant followed the same endocytic pathway as HOLD254, with 60 to 70% LAMP-1- and LAMP-2-positive (data not shown). We also conducted an assay of phagosome-lysosome fusion, at the ultrastructural level, using electron microscopy. BSA-gold was used as a pinocytic, fluid-phase marker of the endosomal-lysosomal pathway. BSA-gold was accumulated mainly in lysosomes after endocytosis of the conjugate-containing medium overnight at 37°C, followed by a chase period of 3 h at 37°C in conjugate-free medium as previously described (33). After a pulse with *L. dumoffii* strains and another chase for 4 h, electron microscopy counting of *L. dumoffii*-containing phagosomes that fused with BSA-gold-labeled lysosomes was performed to assess fusion (Fig. 5). Wild-type-strain-containing phagosomes did not fuse with BSA-gold-marked lysosomes (Fig. 5A). Quantitation showed that only 11.4% (24 of 210) of the phagosomes containing the wild-type strain fused with BSA-gold-marked lysosomes. On the other hand, 85% (187 of 220) of the phagosomes containing the *djlA* mutant strain accumulated BSA-gold (Fig. 5B). Thus, the *djlA* mutant was not able to evade phagosome-lysosome fusion.

Recruitment of the RER. In mammalian macrophages and protozoa, *L. pneumophila* replicates intracellularly in specialized vacuoles surrounded by the RER of the host cells (25, 32). To determine the intracellular location of *L. dumoffii*, we examined J774 macrophages infected with wild-type and *djlA* mutant *L. dumoffii* by using transmission electron microscopy. At 8 h postinfection, the RER around 61 (37.2%) of 164 phagosomes containing wild-type strains were recruited (Fig. 6A) whereas we could not find any phagosomes containing the *djlA* mutant surrounded by RER or attached directly by ribosomes (0 of 153 phagosomes). This was also the case at 24 h (Fig. 6B and data not shown). Phagosomes containing *djlA* mutant cells appeared to harbor much debris, resulting from fusing lysosomes with these vacuoles, while phagosomes containing wild-type cells did not have any contents other than replicating *L. dumoffii* cells (Fig. 6). At 24 h postinfection, many phagosomes containing wild-type cells were broken and their inhabiting macrophages were lysed (data not shown).

Susceptibility of the *djlA* mutant to stress stimuli. In eukaryotic host cells, intracellular pathogens encounter hostile conditions such as toxic oxygen or nitrogen derivatives, intraphagosomal acidification, and harsh degradative enzymes (54, 62). As mentioned above, *djlA* is essential for intracellular growth of *L. dumoffii*. Thus, we examined whether the *djlA* mutant has an increased susceptibility to different environmental stresses. Since previous publications (12, 29) had demonstrated that *L. pneumophila* induces stress resistance in the stationary phase, *L. dumoffii* strains were grown to the stationary phase in BYE medium and subjected to acid shock, oxidative stress, osmotic stress, and heat shock (pH 3 for 5 min, 10 mM H_2O_2 for 30 min, 5 M sodium chloride for 30 min, and 48°C for 60 min, respectively). Compared to the wild-type strain, there was an elevated susceptibility to all stress conditions of the *djlA* mutant strain. There was an increase in the sensitivity of the mutant of 9.8-, 7.4-, 2.6-, and 1.6-fold on exposure to oxidative stress, osmotic stress, heat shock, and acid shock, respectively (Fig. 7). These results suggest that DjlA participated in the protection of *L. dumoffii* on exposure to environmental stress. In the *djlA*-complemented strain, in contrast, resistance to all stress stimuli was restored. The variability in the degree of complementation may result from the different expression of genes from the plasmid and the chromosome.

Presence of *djlA* in other *Legionella* spp. To determine whether *djlA* is also present in nonpathogenic *Legionella* species, PCR amplification with primers in the *djlA* gene was performed for 17 different *Legionella* strains. All the strains used in this experiment are listed in Table 2. The expected 790-bp band was observed in all *Legionella* strains tested except *L. jordanis* and *L. adelaidensis*, irrespective of whether the strain was pathogenic (data not shown). Thus, *djlA* is not unique to particular *Legionella* strains.

DISCUSSION

Legionella spp. are facultative intracellular bacteria that overcome host cell defenses. Although many studies have been

A

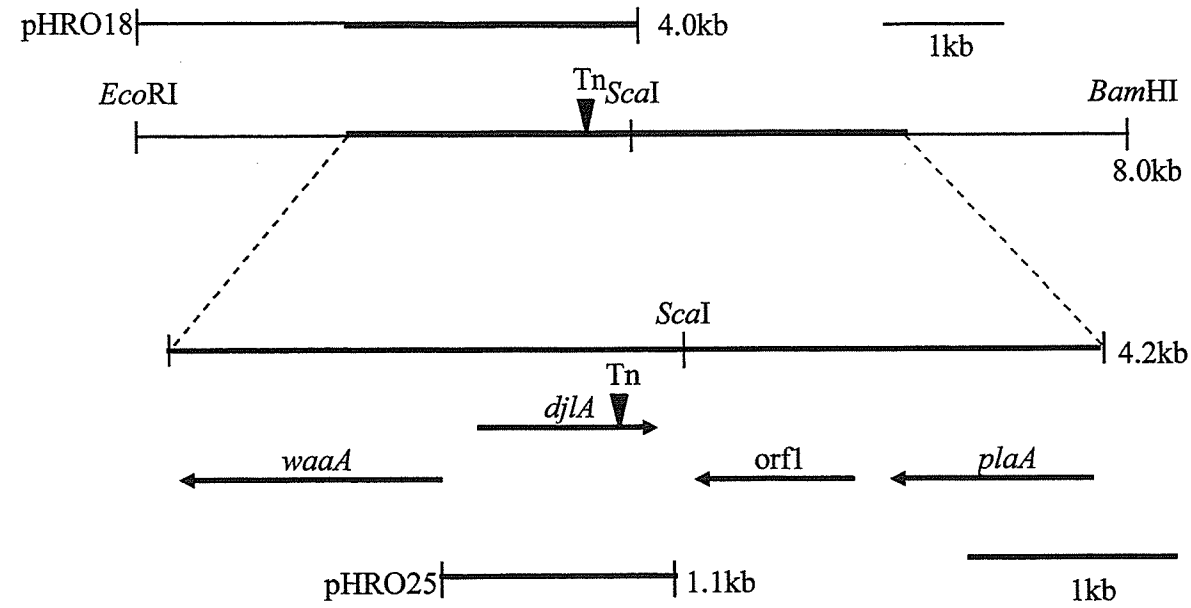

B

TMD

```
L. d MSLRDFFIITTWWGKIIGAFFGYLIAGPT-GAIFGLLVGNFFDRGLYNYFSNPHWLYYTEKRRAIQKIFFEA-TFLV 75
L. p MNLRDFFVITTWWGKILGAFFGYLTAGPV-GALFGILVGNFFDRGLVSYYSNPHWLYHAEKQRIVQKAFFEA-TFSI 75
E. c          MQYWGKIIGVAVALLMGGGFWGVVLGLLIGHMFDKAR----SRKMAWF-A-NQRERQ-AFF-ATTFEV 61

L. d MGHLAKADGRVSEQELDMAR-LFMDEMRLNGEQKTLAKHLFNEGKQSRFNLDSLLENLKKT--CKDNRDLLRLFI-D 148
L. p MGHVAKSDGRVSEQEISMAKSI-MNEMKLSKGQKDLAKRLFNEGKQADFNV-SL-ALIQLQRICKDNRDLLKLFV-D 148
E. c MGHLTKSKGRVTEADIHIASQL-MDRMNLHGASRTAAQNAFRVGKSDNYPLREKMRQ-FRSVCFGRFDLIRMFLEIQ 136

L. d IQYRAAQADG-LDSKKILLLDKIFSRLGFAPLHNQYRFYEDFGRSYSEPQYNTQEQP-QQSRQSQQSDSSSHSYSSY 223
L. p IQYRAAQVDG-LSSQKIHALDNIFTHLGFAPLHKQYRFYEDFG-SYFQQEQSKQHYHNQQEYKHT---SSSQG-QQG 219
E. c IQ--AAFADGSLHPNERAVLYVIAEELGI--SRAQFDQFLRMM----QGGAQFGGGYQQQT-------GGGNW-QQA 197
```

J-domain

```
L. d SRYNYQPTKNNMDYAFALLEVSPKASKQEVKKAYRRLLSRNHPDKLIAQGLPQEMIKMANEKTQKIVKAYELICESKGW 302
L. p YKP-QSPPNTLA-HAFALLEVSPNANKQEVRRAYRRLLSRNHPDKLIAQGLPEEMIKLANDKTHQIMKAYELICETKGWX 296
E. c QRG---P--TLE-DACNVLGVKPTDDATTIKRAYRKLMSEHHPDKLVAKGLPPEMMEMAKQKAQEIQQAYELIKQQKGFK 271
```

FIG. 3. Chromosomal arrangement of the region surrounding the *djlA* gene and sequence alignment of DjlA proteins. (A) At the top is a plasmid used for complementation studies (pHRO18) and an 8-kb region of the *L. dumoffii* cosmid clone including the *djlA* gene, along with the location of relevant restriction enzyme sites. The thick line represents the DNA region that we sequenced. Below these diagrams, the distance between the *djlA* gene and neighboring genes and the orientation and size of the transcribed genes are delineated by the arrows below the 4.2-kb sequenced region. Another plasmid used for complementation studies (pHRO25) is also shown. The site of the Tn*903*dI*lacZ* insertion (Tn) is indicated by the inverted arrowhead. The full names of the gene mapped are as follows: *waaA*, Kdo transferase gene; *djlA*, *dnaJ*-like A gene; *plaA*, lysophospholipase A gene. Orf1 is a putative open reading frame which showed no homology to known genes. (B) Sequence similarity of the predicted Dj1A protein of *L. dumoffii* (L.d, top line), *L. pneumophila* (L.p, middle line) and *E. coli* (E.c, bottom line). Amino acid residues conserved in the three sequences, appear in bold type. Gaps marked by dashes are introduced to reveal the maximal similarity among the sequences. The C-terminal J-domain and the N-terminal TMD are shown schematically above the sequences.